CONFIDENTIAL AUG 2 3 1954

Copy 74
RM L50H15

NACA RM L50H15

AERONAUTICS LIBRARY
California Institute of Technology

NACA

RESEARCH MEMORANDUM

LOW-SPEED INVESTIGATION OF A SEMISUBMERGED AIR SCOOP WITH AND WITHOUT BOUNDARY-LAYER SUCTION

By P. Kenneth Pierpont and Robert R. Howell

Langley Aeronautical Laboratory
Langley Field, Va.

CLASSIFIED DOCUMENT

This document contains classified information affecting the National Defense of the United States within the meaning of the Espionage Act, USC 50:31 and 32. Its transmission or the revelation of its contents in any manner to an unauthorized person is prohibited by law.

Information so classified may be imparted only to persons in the military and naval services of the United States, appropriate civilian officers and employees of the Federal Government who have a legitimate interest therein, and to United States citizens of known loyalty and discretion who of necessity must be informed thereof.

NATIONAL ADVISORY COMMITTEE
FOR AERONAUTICS

WASHINGTON

February 23, 1951

CONFIDENTIAL

NATIONAL ADVISORY COMMITTEE FOR AERONAUTICS

RESEARCH MEMORANDUM

LOW-SPEED INVESTIGATION OF A SEMISUBMERGED AIR SCOOP WITH AND WITHOUT BOUNDARY-LAYER SUCTION

By P. Kenneth Pierpont and Robert R. Howell

SUMMARY

A preliminary low-speed investigation has been made of an air scoop submerged one-half the inlet height in a depression on the surface of a simulated fuselage. Boundary-layer suction was used on the steep approach ramp to improve the internal flow. A 6°-included-angle diffuser with an area ratio of 1.9:1 was located behind the inlet in the model. Most of the tests were conducted with an initial turbulent boundary layer believed to approximate that which would occur on the forward part of a fuselage. A few tests were made with a boundary layer about 2.5 times the thickness of the original boundary layer to determine the effect of moving the inlet farther rearward on the fuselage. The effects of suction-slot location and slot width were determined and a few tests with area suction were made. The maximum quantity of suction flow was about 15 percent of the inlet flow at an inlet-velocity ratio of 0.6.

Gains up to about 8 percent in the impact-pressure ratio at the end of the diffuser were obtained with suction; at the same time, the inlet-velocity ratio for maximum recovery was observed to shift from about 0.75 to 0.55. For the configurations tested, area suction and suction slots were about equally effective. The impact pressure inside the slot was markedly increased with an increase in slot width; slot static pressures indicated that choking at high forward speeds is not likely to occur with the wide slot. The critical Mach number for the inlet was limited by the external lip to 0.78 at an inlet-velocity ratio of 0.6; the critical Mach number of the other inlet components was greater than 0.8. Approximate incremental increases in inlet impact-pressure ratio, calculated by integrating the total-pressure distributions immediately ahead of the approach ramp, were found to be in good agreement with experimental values. The impact-pressure ratio of the partly submerged inlet exceeded that of the submerged inlet in the inlet-velocity-ratio range suitable for high-speed operation.

INTRODUCTION

Much interest has been shown in fuselage submerged scoop inlets because of the necessity of placing such items as guns, radar equipment, and cameras in the fuselage nose. Reference 1 describes a low-speed investigation of one proposed design in which the air scoop is completely submerged in a depression on a simulated fuselage. Boundary-layer suction was used for this configuration both on the approach ramp and inside the diffuser. Such complete submergence of the inlet within the basic fuselage line is considered desirable to reduce the frontal area and to prevent the entrainment of foreign material in the inlet. It becomes difficult to obtain high impact-pressure ratios with such a design, however, without the use of excessive boundary-layer suction and some compromise may generally be required. Accordingly, the present tests were undertaken to study the effects of boundary-layer suction on the impact-pressure ratio of a scoop similar to that of reference 1 except that it was half submerged.

Impact-pressure ratios at the inlet and at the end of the diffuser were obtained for a range of inlet-velocity ratios from about 0.3 to 1.5 and for various amounts of suction, less than about 15 percent of the inlet flow at an inlet-velocity ratio of 0.6, applied at discrete slots or over areas of porous material. Static-pressure distributions over the external and internal surfaces were measured and the impact-pressure ratio in the suction slot was determined for two representative slots.

SYMBOLS

a	distance normal to surface, determined from $\left(C_Q\delta^* = \int_0^a \left(\frac{V}{V_o}\right) dy\right)$, inches
b	span of slot, inches
d	equivalent-nose-inlet inside diameter, inches (2h)
D	equivalent-nose-inlet outside diameter, inches (2(h + Y))
H	total pressure, pounds per square foot
h	inlet height measured perpendicular to duct center line at minimum area, inches
h'	effective height of entering air layer, inches $\left(h\left(\frac{V_i}{V_o}\right) + \delta^*_a\right)$

p	static pressure, pounds per square foot
q	dynamic pressure, pounds per square foot
Q	volume rate of flow, cubic feet per second
V	velocity, feet per second
x	distance parallel to X-axis, positive behind scoop lip, inches (see table I and figure 3)
y	distance parallel to Y-axis, positive above surface, inches (the Y-axis is normal to a plane tangent to fuselage at center line of inlet, see table I and figure 3)
z	distance parallel to Z-axis, inches (the Z-axis is in tangent plane and is perpendicular to center line, see table I and figure 3)
C_Q	suction-flow coefficient $\left(Q_s/b\delta^*V_o\right)$
H'	boundary-layer shape parameter (δ^*/θ)
P	static-pressure coefficient $\left(\frac{p - p_o}{q_o}\right)$
δ	boundary-layer thickness, inches
δ^*	boundary-layer displacement thickness, inches $\left(\int_0^\delta \left(1 - \frac{V}{V_o}\right) dy\right)$
δ^*_a	boundary-layer displacement thickness outboard of a, inches $\left(\int_a^\delta \left(1 - \frac{V}{V_o}\right) dy\right)$
θ	boundary-layer momentum thickness, inches $\left(\int_0^\delta \left(1 - \frac{V}{V_o}\right)\frac{V}{V_o} dy\right)$
y'	inlet-lip ordinate, inches
r	leading-edge radius, inches
X_l	distance from leading edge to maximum equivalent-nose-inlet outside diameter, inches
Y_l	maximum inlet-lip ordinate, inches

Subscripts:

1	conditions at front measurement station
2	conditions at rear measurement station
i	point of minimum area near entrance
o	free-stream conditions
s	conditions at suction slot
av	average value weighted according to local velocity in the main duct
min	minimum

APPARATUS AND TESTS

A diagrammatic sketch of the test setup is shown in figure 1 and photographs of two of the configurations are presented in figure 2. Transverse and longitudinal contour lines are shown in figure 3 and surface ordinates are given in table I. Line drawings of the boundary-layer-removal systems are given in figure 4.

The inlet had an area of 26.3 square inches measured in a plane perpendicular to the duct center line with a ratio of span to maximum height of about 3.6. At the end of the 7-inch-long constant-area entrance section, the upper and lower walls of the diffuser diverged with an included angle of 6° to provide an area-expansion ratio of 1.9:1 to the rear measurement station. The inner and outer lip shapes were laid out from the nose-inlet data of reference 2 and may be considered to be equivalent-nose-inlet contours if an equivalent inside diameter is defined as twice the inlet height (2h) measured normal to the duct center line and an equivalent outside diameter as twice the sum of the inlet height and the lip thickness (2h + 2Y). Ordinates for the inlet lip and afterbody are given in tables II(a) and II(c). The outside lip shape was modified after initial tests according to table II(b) in order to reduce the magnitude of the surface-pressure coefficient.

Four 12-inch-span flush-type suction slots (fig. 4(a)) and two areas of porous material (fig. 4(b)) were tested. Slots I and II were vertical slots with rounded corners, whereas slots III and IV were inclined to the surface and included a diffuser. The porous material consisted of 40-mesh bronze hardware cloth hammered to a thickness of 0.019 inch and mounted on a perforated steel plate. The square of the normal velocity through

the material was numerically equal to 4.08 times the pressure drop in pounds per square foot across the screen. Visual inspection of the cloth indicated that the hole size and spacing was adequately uniform.

Pressures at the entrance and end of the diffuser of the main duct and in the boundary-layer slots were measured by means of the rakes of total- and static-pressure tubes shown in figure 5. The inlet rake of the main duct (fig. 4(b)) was always removed when pressures were measured at the end of the diffuser. Surface pressures were obtained by the use of flush orifices. Boundary-layer surveys ahead of the inlet were obtained with a total- and static-pressure probe. The outside diameter of the total-pressure tube was 0.030 inch (0.002-inch wall thickness) and was flattened to 0.012-inch over-all thickness; the static-pressure tube had an outside diameter of 0.040 inch.

Inlet- and suction-flow quantities were measured with the aid of calibrated venturis. Differential venturi pressures, together with tunnel stagnation pressure, were measured on kerosene-filled micromanometers. All pressure measurements on the model were recorded photographically on a vertical alcohol-filled multiple-tube manometer. Tufts were used to observe the direction and stability of the flow.

Each of the inlet configurations was tested in conjunction with one or both of the two boundary layers 14.5 inches ahead of the scoop lip shown in figure 6. Boundary layer A was obtained by shellacking an 8-inch band of screened sand (20-mesh hardware cloth) to the floor forward of the 34-inch station; boundary layer B was generated by placing $\frac{1}{4}$-inch-diameter rods transversely on the surface immediately ahead of and behind the sand strip. In each case, modifications were made in the distribution of the sand or in the positions of the rods until a reasonably uniform boundary layer was obtained transversely over the body. Values of the displacement thickness δ^* and shape parameter H' at the center line are 0.092 and 1.26, respectively, for boundary layer A and 0.214 and 1.25 for boundary layer B.

All tests were conducted in the $\frac{1}{15}$-scale model of the Langley full-scale tunnel at a speed of about 100 feet per second which corresponds to a Reynolds number of approximately 1.5×10^5 based on the inlet height.

RESULTS AND DISCUSSION

All the results discussed, unless otherwise noted, are those obtained with boundary layer A since it was believed to approximate that on the forward part of a fuselage. The boundary-layer suction coefficient, $C_Q = Q_s/V_o\delta^* b$, is the ratio of the quantity of flow entering the slot to the quantity of flow displaced by the boundary layer 14.5 inches ahead

of the inlet. This coefficient is used as a parameter instead of the ratio of the suction flow to the flow quantity in the main duct because it is independent of the inlet-velocity ratio. The boundary-layer suction flow for boundary layer A expressed in percent inlet flow is numerically equal to $4C_Q/(V_i/V_o)$; thus, at $\frac{V_i}{V_o} = 0.6$ and $C_Q = 0.9$, the suction flow is 6 percent of the inlet flow.

Flow at the Inlet

Average impact-pressure ratios, weighted according to local velocity, are shown as a function of inlet-velocity ratio at the scoop inlet in figure 7 for the ramp without suction and with suction slots I, II, and III. For the no-suction case, 100 percent free-stream impact pressure was never realized at any inlet-velocity ratio because of the losses associated with the entering boundary layer. Separation ahead of the front measuring station, which was observed with tufts, caused the abrupt decrease in impact-pressure ratio below $\frac{V_i}{V_o} = 0.5$. At $\frac{V_i}{V_o} = 0.3$ separation started 4 or 5 inches ahead of the inlet. Boundary-layer suction, applied ahead of the initial separation, reduced the extent of separation so that, for $\frac{V_i}{V_o} = 0.4$ and suction-flow coefficient greater than 0.9, the impact-pressure recovery exceeded $0.88q_o$ for all slots.

Comparison of figures 7(b), 7(c), and 7(d) for the three suction slots shows that, to obtain high recovery at the inlet, the slot location was critical only for inlet-velocity ratios less than about 0.5. For the moderate to high inlet-velocity ratios, the position of the suction slot had no pronounced effects, at least in the range of slot positions tested. At an inlet-velocity ratio of 0.6, an increase in impact-pressure recovery of about $0.05q_o$ is shown for the highest suction quantity; this increase was about 15 percent of the flow entering the main duct.

Representative velocity contours at the front measurement station have been plotted in figure 8(a) for $\frac{V_i}{V_o} = 0.6$ with no suction and for $C_Q = 1.35$ and 2.39. Similar contours at the rear measurement station are shown in part (b) of this figure. The dissymmetry of the flow shown in figure 8 may have resulted from some initial nonuniformity in the flow along the floor ahead of the inlet, lack of geometric symmetry, or nonuniform distribution of the flow into the suction slot.

Flow in the Diffuser

Without boundary-layer control, tuft surveys showed that separation from the top and end sections did not occur but that all separation, when it occurred, took place on the bottom of the diffuser. Separation was indicated ahead of the inlet on the ramp below inlet-velocity ratios of about $\frac{V_i}{V_o} \approx 0.5$ and, as the inlet-velocity ratio was increased, it moved progressively rearward until it passed the rear measurement station at an inlet-velocity ratio of about $\frac{V_i}{V_o} \approx 1.2$. When boundary-layer suction was applied with a suction slot ahead of the inlet and sufficient suction flow was used, separation began much farther rearward and, for $C_Q > 2.0$, did not occur ahead of the rear measurement station above $\frac{V_i}{V_o} \approx 0.8$. The impact-pressure ratio without boundary-layer control is shown in figure 9(a) as a function of inlet-velocity ratio. Comparison of this figure with figure 7(a) shows the relatively large losses (in percent of inlet q) that occurred due to separation of the ramp flow at the low inlet-velocity ratios. For example, at $\frac{V_i}{V_o} = 0.4$ $\left(\text{nominal } \frac{q_i}{q_o} = 0.16\right)$, figures 7(a) and 9(a), show a loss of $0.10q_o$ or about 60 percent mean inlet q is shown. The maximum impact-pressure recovery was reached at about $\frac{V_i}{V_o} = 0.80$ and was approximately $0.85q_o$. Beyond this value of V_i/V_o, the recovery decreased slowly to $0.69q_o$ at $\frac{V_i}{V_o} = 1.50$.

With suction applied on the ramp ahead of the inlet for slots I, II, or III, the impact-pressure ratios are shown in figures 9(b), 9(c), and 9(d), respectively. Velocity distributions at the rear measurement station can be seen in figure 8(b) for $\frac{V_i}{V_o} = 0.6$ for no suction, $C_Q = 1.35$, and $C_Q = 2.39$. Because of the shift in the separation, the value of V_i/V_o for the maximum recovery moved to lower inlet-velocity ratios so that, for $C_Q \approx 2.3$, the highest value tested, the maximum impact-pressure recovery was about $0.93q_o$ and occurred between $\frac{V_i}{V_o} = 0.5$ and $\frac{V_i}{V_o} = 0.65$ for all slots. This maximum recovery represents an increase of about 8 percent above the maximum obtained without suction. For a given suction quantity, the maximum recovery shifted to higher inlet-velocity

ratios for slot II than for slot I; however, for slot III, the maximum recovery occurred at about the same inlet-velocity ratio as for slot II.

For the high inlet-velocity ratios, the curves for different suction quantities tend to converge. This convergence could be foreseen since at the highest velocity ratios no separation existed and the increased losses were nearly constant and equal to about $0.08q_i$. Thus, boundary-layer suction may not be justified for inlet-velocity ratios greater than about $\frac{V_i}{V_o} = 0.7$.

The results of two tests with area suction are shown in figure 10. The inlet-velocity ratio indicated for these tests is determined by the flow quantity after diffusion; consequently, the true inlet-velocity ratio is about $0.04C_{Q_2}$ higher when area II was used. These tests were included to determine whether large flow improvements could be obtained with porous suction but, because of the large porosity of the material, are not considered conclusive. No significant changes in impact-pressure ratio occurred with a change in suction quantity. The maximum recovery occurred at about $\frac{V_i}{V_o} = 0.6$ and was $0.92q_o$ or about 1 percent less than with a suction slot for the same suction flow. The flow quantities for the two suction regions were controlled separately for two conditions which gave a total-flow quantity $C_{Q_1} + C_{Q_2} \approx 2.3$. With the forward area handling the larger suction flow, the pressure recovery was constantly higher than when the rear area was handling the larger suction flow. The curve for $C_Q = 2.3$ is almost the same as that for the single slot III for the same total suction flow, and the maximum recovery was 0.94 which is 1 percent higher than for slot III. This small gain is not surprising since the continuous removal of the low-energy air would probably result in a slightly thinner boundary layer at the end of the suction region than would a single slot located at the front of the porous area, provided separation did not occur for either case. For the conditions of these tests, area suction and suction slots were about equally effective.

Impact-pressure ratio after diffusion with boundary layer B is shown as a function of inlet-velocity ratio in figure 11 for slots III and IV. It is readily seen that the slot width had little effect on the impact-pressure ratio. The suction coefficient was approximately unity based on the displacement thickness of boundary layer B or is equivalent to about $C_Q = 2.5$ based on boundary layer A. The maximum recovery shown is $0.82q_o$ and occurred at an inlet-velocity ratio of 0.85. It is apparent from the low impact-pressure ratio that a suction-flow coefficient of 1.0 was too low for adequate removal of boundary layer B. It may be expected that a suction-flow coefficient of at least 2.4, based

on the displacement thickness at boundary layer B, would be required to obtain a maximum impact-pressure recovery comparable to the maximum obtained with boundary layer A. Impact-pressure recoveries with greater suction flows were not obtained since, to obtain a suction-flow coefficient $C_Q = 2.4$, more than 40 percent of the inlet flow at $\frac{V_i}{V_o} = 0.6$ would be required.

Surface Pressures

Distributions of surface pressure along the center line of the ramp from a position near the crest of the ramp to about 20 inches inside the diffuser are shown in figures 12(a) and 12(b) for slot III, $C_Q = 2.39$, and for slot IV, $C_Q = 2.29$, respectively, for four representative inlet-velocity ratios. Inlet-velocity ratio had little effect on the pressures near the ramp crest ($x = -12.75$ in.) but had a marked effect in the vicinity of the suction slots. The sudden pressure rise across slot III $\left(\approx 0.5q_o \text{ at } \frac{V_i}{V_o} = 0.64 \text{ fig. 12(a)}\right)$ is the characteristic sink effect and was less for the wider slot IV. Immediately behind the slot, the pressure changed rapidly to meet the entrance conditions determined by inlet-velocity ratio and losses in total pressure on the ramp and then increased slowly to the end of the diffuser.

Figure 12(c) shows the variation of surface pressure coefficient in the vicinity of, and within slot III, for several suction-flow rates at a nominal inlet-velocity ratio of 0.6; in addition, one curve for slot IV is shown. Because of the large negative pressures inside slot III ($P = -2.28$ at $C_Q = 2.39$), slot choking will probably occur at high forward speeds, whereas slot IV ($P = 0.08$ at $C_Q = 2.29$) will operate satisfactorily. The longitudinal variation of surface pressures for the valley or gutter is shown in figure 13 and for the ridge or outer edge of the depression in figure 14 for slot III operating at a suction-flow coefficient of 2.39. Because the pressures on the duct center line were more positive than those in the gutter (compare fig. 13 with fig. 12(a) forward of the inlet), it is believed that an excessive amount of boundary-layer air was not taken into the inlet at low inlet-velocity ratios. Also, the pressure differences between the gutter and the ridge behind the slot tend to direct the boundary layer outward from the gutter to the ridge; this outward flow in the boundary layer was observed with tufts.

Pressure distributions over the inside and outside surfaces of the original and modified lip at the center line are shown in figures 15(a) and 15(b). No large negative pressure peaks and consequently no high

induced local velocities were present near the outside lip leading edge for either configuration. The minimum pressures on the outside of the lip occurred 3 to 4 inches behind the leading edge; this point was very nearly maximum thickness. The external-lip modification shown in figure 4(a) resulted in a reduction in the maximum negative pressure from $-0.35q_o$ to $-0.28q_o$ at an inlet-velocity ratio of 0.64; this reduction was accompanied by a slight increase in the magnitude of the negative pressures near the lip. At high inlet-velocity ratios a sharp negative pressure peak occurred on the inside lip; however, separation was not indicated by the pressure distributions (fig. 15) and large reductions in impact-pressure ratio were not observed even at the maximum test inlet-velocity ratio (see fig. 9). Pressure distributions on the top corner and end of the inlet lip, parts (c) and (d) of figure 15, were, in general, similar to those at the center line and no severe pressure peaks were observed.

To gain some insight into the high-speed performance of the inlet, curves of the maximum negative pressure coefficient for the several components are shown in figure 16. Within the probable high-speed operating range from $\frac{V_i}{V_o} = 0.45$ to 0.7, the predicted critical Mach number is controlled by the outside of the lip; pressures on the other components remained greater than $-0.25q_o$ which corresponds to a critical Mach number, calculated according to the von Kármán method, of about 0.8. The maximum local velocities on the lip may be decreased by the use of a thinner lip shape; however a sharp localized peak may occur on the nose for the high-speed inlet-velocity ratios. Tests of nose inlets at subcritical and supercritical speeds (reference 3) indicate that such localized peaks do not necessarily result in large increments in drag.

All the surface-pressure coefficients and the minimum pressure coefficients shown in figure 16 may not be conservative because the reference static pressure corresponds to the static pressure near the air scoop on a complete fuselage. If the pressures on a fuselage near the inlet are free stream, then the pressures shown will give the correct critical Mach number.

Remarks on Suction Performance

The required width of the suction slots for this investigation was estimated to be about twice the displacement thickness of the boundary layer 14.5 inches ahead of the inlet (reference 4). Slots III and IV were inclined 30° with respect to the tunnel floor and had an approximately 2:1 area ratio diffuser to recover some of the dynamic pressure. Impact-pressure ratio for these two slots is shown plotted against inlet-velocity ratio in figure 17. For the conditions shown, the curves

are approximately linear and the slope of the curves is not considered excessive. At $\frac{V_i}{V_o} = 0.6$ and $C_Q = 2.39$, slot III gave a recovery of $0.18q_o$; widening the slot (slot IV) for nearly the same flow coefficient ($C_Q = 2.29$) resulted in a recovery greater than $0.40q_o$. For a complete installation, this increased recovery represents a marked reduction in pumping power. Also shown in figure 17 is a single curve for the recovery in slot IV for boundary layer B, for which $C_Q = 0.92$. Spanwise distributions of impact-pressure ratio 1/2 inch inside slots III and IV are shown in figure 18 for several suction-flow rates with boundary layer A and for one condition with boundary layer B.

Remarks Concerning the Impact Pressure Available at the Inlet

The impact pressure available at the inlet of a scoop is governed by the initial boundary layer ahead of the inlet. Even with a knowledge of the static-pressure distribution in a three-dimensional-flow field such as exists on a fuselage with an air scoop, calculation of the impact-pressure ratio is at present not feasible. Lacking the means to calculate the mean impact pressure available at the inlet, an upper limit to the impact-pressure ratio can be established provided the boundary layer on the fuselage immediately ahead of the inlet-flow field is known. Some of the effects of initial boundary-layer thickness and boundary-layer suction can also be shown. The upper limit of the impact-pressure ratio can be expressed in terms of a known boundary-layer profile close to the inlet in the form

$$\frac{H_1 - p_o}{H_o - p_o} = \frac{\int_a^{h'} \left(\frac{V}{V_o}\right)^3 dy}{\int_a^{h'} \left(\frac{V}{V_o}\right) dy} \tag{1}$$

The lower integration limit is determined by the suction applied and is found from

$$C_Q \delta^* = \int_0^a \left(\frac{V}{V_o}\right) dy \tag{2}$$

The upper limit of the integration is determined from the inlet-velocity ratio, the inlet height, the initial displacement thickness, and by the amount of suction applied. Thus

$$h' = h \frac{V_i}{V_o} + \delta^*_a \tag{3}$$

where

$$\delta^*_a = \int_a^{\delta} \left(1 - \frac{V}{V_o}\right) dy \tag{4}$$

For the case of no suction, a is zero and δ^*_a is the displacement thickness of the initial boundary layer. Illustration of the definition of the terms is given in figure 19.

The theoretical upper limit of impact pressure available at the inlet was calculated from equation (1) by using the boundary layer 14.5 inches ahead of the inlet and is plotted as a function of inlet-velocity ratio in figure 20 for rates of suction flow comparable to those used in the tests. For a suction-flow coefficient of $C_Q = 2.25$, the calculated increases in the upper limit of the impact pressure available at the inlet for inlet-velocity ratios of $\frac{V_i}{V_o} = 0.6$ and 1.5 are 5 percent and 2 percent, respectively. In order to compare these increments with the experimental results, the most forward suction slot was selected as most nearly corresponding to the assumed conditions. From figures 7(a) (no suction) and 7(d) (slot III, $C_Q = 2.39$) the incremental increase in recovery is seen to be, for inlet-velocity ratios of 0.6 and 1.5, about 5 and 2 percent, respectively. This agreement is considered to be of value in assessing the effects of boundary-layer suction.

With no suction, the theoretical upper limit of the impact pressure available at the inlet for boundary layer B is considerably less than that for boundary layer A, and the data of figure 20 show that a larger suction flow, proportional to the displacement thickness of the boundary layer, is required to obtain the same impact-pressure ratio for boundary layer B as for the thinner boundary layer A. For example, a suction-flow coefficient of $C_Q = 2.25$ is required for boundary layer B ($\delta^* = 0.214$ in.) to obtain approximately the same recovery as $C_Q = 0.9$ for boundary layer A ($\delta^* = 0.092$ in.).

Comparison of Performance of the Semisubmerged Scoop with a Similar Fully Submerged Scoop

In order to compare the performance of the semisubmerged air scoop of the present investigation ($\delta^* = 0.092$ in.) with that of the submerged air scoop of reference 1 ($\delta^* = 0.085$ in.), impact-pressure ratios at the inlet and after approximately 2:1 diffusion are shown in figure 21 without suction and for a suction-flow coefficient of $C_Q = 1.7$. The impact-pressure recovery of the semisubmerged scoop at the inlet and after diffusion exceeds the recovery of the submerged scoop for inlet-velocity ratios less than about 1.0 with or without boundary-layer suction; however, for higher inlet-velocity ratios, the recovery at the semisubmerged scoop is less than that of the submerged scoop of reference 1.

The improved recovery of the semisubmerged inlet over the submerged inlet at inlet-velocity ratios corresponding to high-speed operating conditions probably arises from the fact that the semisubmerged scoop was attained by moving the inlet lip forward along the approach ramp from the submerged position to a position required by semisubmergence. The inlet-positive-pressure field in this case reduced the static-pressure rise required by reducing the maximum negative pressures near the crest of the ramp. Figure 21 shows that for the semisubmerged inlet with no suction, the impact-pressure recovery for an inlet-velocity ratio of 0.6 is $0.09q_o$ greater than that for the model of reference 1, even though the displacement thickness of the boundary layer measured at the same position relative to the crest of the ramp for the present test was greater.

A comparison of the performance of the two inlets has been made in terms of the changes in net thrust and specific fuel consumption at $\frac{V_i}{V_o} = 0.6$ with no boundary-layer control and also with a suction-flow coefficient of $C_Q = 1.7$ for an assumed 4,000-pound-thrust turbojet engine operating at a Mach number 0.9 at 40,000 feet altitude. In these calculations the external drags have been assumed to be equal. The following table shows the net change in percent thrust and specific fuel consumption based on an inlet operating at an impact-pressure ratio of 1.0.

Configuration	C_Q	$\frac{H_2 - p_o}{H_o - p_o}$	Percent change in NT	Percent change in SFC
No slot	0	0.82	-10.8	3.9
Slot IV	1.7	.90(est.)	-8.4	1.9
Configuration I (reference 1)	0	.74	-15.8	6.2
Configuration V (reference 1)	1.7	.86	-11.3	3.0

For the condition of no-boundary-layer suction, the semisubmerged air scoop gave a 5-percent improvement in net thrust. For the suction coefficient of 1.7 a 2.9-percent increase was obtained. Similarly, the semisubmerged scoop with $C_Q = 1.7$ has 1.1-percent less increase in specific fuel consumption than the air scoop of reference 1 for the same suction-flow rate. High-speed tests of both types of air scoops will be required to fully define their performance.

SUMMARY OF RESULTS

A preliminary low-speed investigation has been made of an air scoop submerged one-half the height of the inlet in a depression on a simulated fuselage. The more important results are summarized as follows:

1. Application of boundary-layer suction by means of a slot located ahead of the inlet increased the impact-pressure ratio at the inlet over the entire range of inlet-velocity ratios studied; the slot position, except at low inlet-velocity ratios, was not found to be critical and suction slots and area suction were found to be about equally effective.

2. With no suction, the impact-pressure recovery was $0.85q_o$ at $\frac{V_i}{V_o} = 0.8$; a suction-flow quantity corresponding to about 15 percent of the inlet flow at $\frac{V_i}{V_o} = 0.6$ increased the impact-pressure recovery to $0.93q_o$ and maximum recovery occurred between inlet-velocity ratios of 0.5 to 0.65 for all slots tested.

3. The impact-pressure ratio in the suction slot at the highest suction-flow rate was increased from about 0.18 with a slot 0.19 inch wide to more than 0.4 with a slot 0.35 inch wide at $\frac{V_i}{V_o} = 0.6$.

4. For the probable high-speed operating range $\left(\frac{V_i}{V_o} = 0.45 \text{ to } 0.75\right)$ the critical Mach number was established by the outside of the inlet lip; for the other components the critical Mach number was estimated to be 0.8.

5. An upper limit to the inlet impact-pressure ratio was calculated by integrating the impact-pressure distributions 14.5 inches ahead of the inlet. Incremental increases in impact-pressure ratio with boundary-layer suction at $\frac{V_i}{V_o} = 0.6$ and 1.5 were calculated to be 5 percent and 2 percent, respectively; these increments agree with the corresponding experimental values.

6. The impact-pressure recovery of the semisubmerged air scoop of the present study is greater than that of a similar fully submerged scoop for the high-speed operating range of inlet-velocity ratios.

Langley Aeronautical Laboratory
National Advisory Committee for Aeronautics
Langley Field, Va.

REFERENCES

1. Nichols, Mark R., and Pierpont, P. Kenneth: Preliminary Investigation of a Submerged Air Scoop Utilizing Boundary-Layer Suction to Obtain Increased Pressure Recovery. NACA RM L50A13, 1950.

2. Baals, Donald D., Smith, Norman F., and Wright, John B.: The Development and Application of High-Critical-Speed Nose Inlets. NACA Rep. 920, 1948.

3. Pendley, Robert E., and Smith, Norman F.: An Investigation of the Characteristics of Three NACA 1-Series Nose Inlets at Subcritical and Supercritical Mach Numbers. NACA RM L8L06, 1949.

4. Pierpont, P. Kenneth: Investigation of Suction-Slot Shapes for Controlling a Turbulent Boundary Layer. NACA TN 1292, 1947.

TABLE I.- LONGITUDINAL SURFACE ORDINATE: y

[All dimensions are in inches]

x \ z	0	4.00	6.00	6.50	8.00
-12.75	0.00	-0.30	-0.68	-0.81	-1.21
-11.75	-.01	-.30	-.68	-.81	-1.21
-10.75	-.04	-.32	-.68	-.81	-1.21
-9.75	-.09	-.36	-.68	-.81	-----
-8.75	-.16	-.38	-.69	-.81	-----
-7.75	-.25	-.42	-.76	-.84	-----
-6.75	-.36	-.52	-.84	-.89	-----
-5.75	-.49	-.63	-.93	-.97	-----
-4.75	-.64	-.76	-1.03	-1.04	-----
-3.75	-.81	-.89	-1.14	-1.14	-1.21
-2.75	-1.00	-1.04	-1.25	-1.25	-1.21
-1.75	-1.21	-1.24	-1.44	-1.40	-1.21
-.75	-1.44	-1.44	-1.54	-1.45	-----
.25	-1.70	-1.70	-.10	-1.31	-----
1.25	-1.98	-2.00	-.60	-.92	-----
2.25	-2.27	-2.28	-.98	-.96	-----
3.25	-2.60	-2.60	-1.14	-.88	-----
4.25	-2.94	-2.94	-1.27	-.71	-----

NACA

TABLE II.- INLET LIP ORDINATES

[All dimensions are in inches]

(a) Equivalent Original Lip

NACA 1-70-090 Cowling

Outside fairing		Inside fairing	
x	y'	x	y'
0.00	0.00	0.00	0.00
.10	.18	.10	-.12
.20	.26	.20	-.20
.30	.33	.30	-.22
.40	.39	.40	-.26
.50	.44	.50	-.30
1.00	.64	1.00	-.43
1.50	.79	1.50	-.53
2.00	.91	2.00	-.61
2.50	1.01		
3.00	1.09		
3.50	1.14		
4.00	1.19		
4.50	1.21		
5.00	1.22		

X_l = 5.00, Y_l = 1.13, r = 0.03

Note: These ordinates measured from lip reference line at plane of symmetry.

(b) Equivalent Modified Lip

NACA 1-70-110 Cowling

Outside fairing		Inside fairing	
x	y'	x	y'
0.00	0.00	0.00	0.00
.15	.19	.10	-.12
.30	.29	.20	-.20
.60	.42	.30	-.22
.90	.55	.40	-.26
1.20	.62	.50	-.30
1.50	.69	1.00	-.43
1.80	.76	1.50	-.53
2.10	.83	2.00	-.61
2.40	.89		
3.00	.97		
3.60	1.04		
4.20	1.10		
4.80	1.14		
5.40	1.16		
6.00	1.17		

X_l = 6.00, Y_l = 1.17, r = 0.03

Inner-lip ordinates become tangent to duct fairing at lip station 0.50.

(c) Afterbody Fairing[1]

x	y
6.00	2.54
8.00	2.50
12.00	2.22
14.00	1.97
16.00	1.81
18.00	1.41
20.00	1.10
22.00	.77
24.00	.44
26.00	.18
26.40	.00

[1] Faired from ℄ of simulated fuselage.

NACA

CONFIDENTIAL

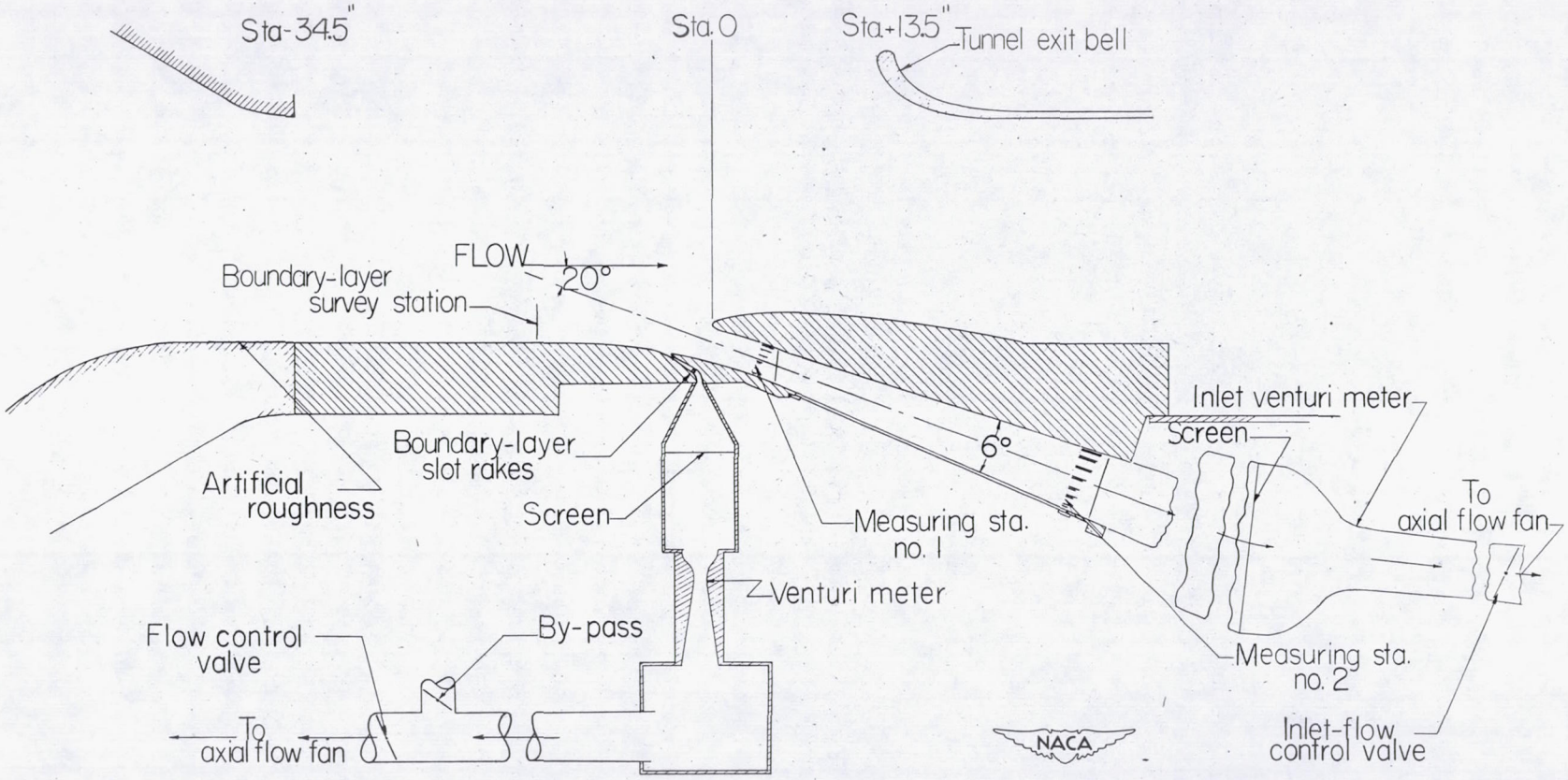
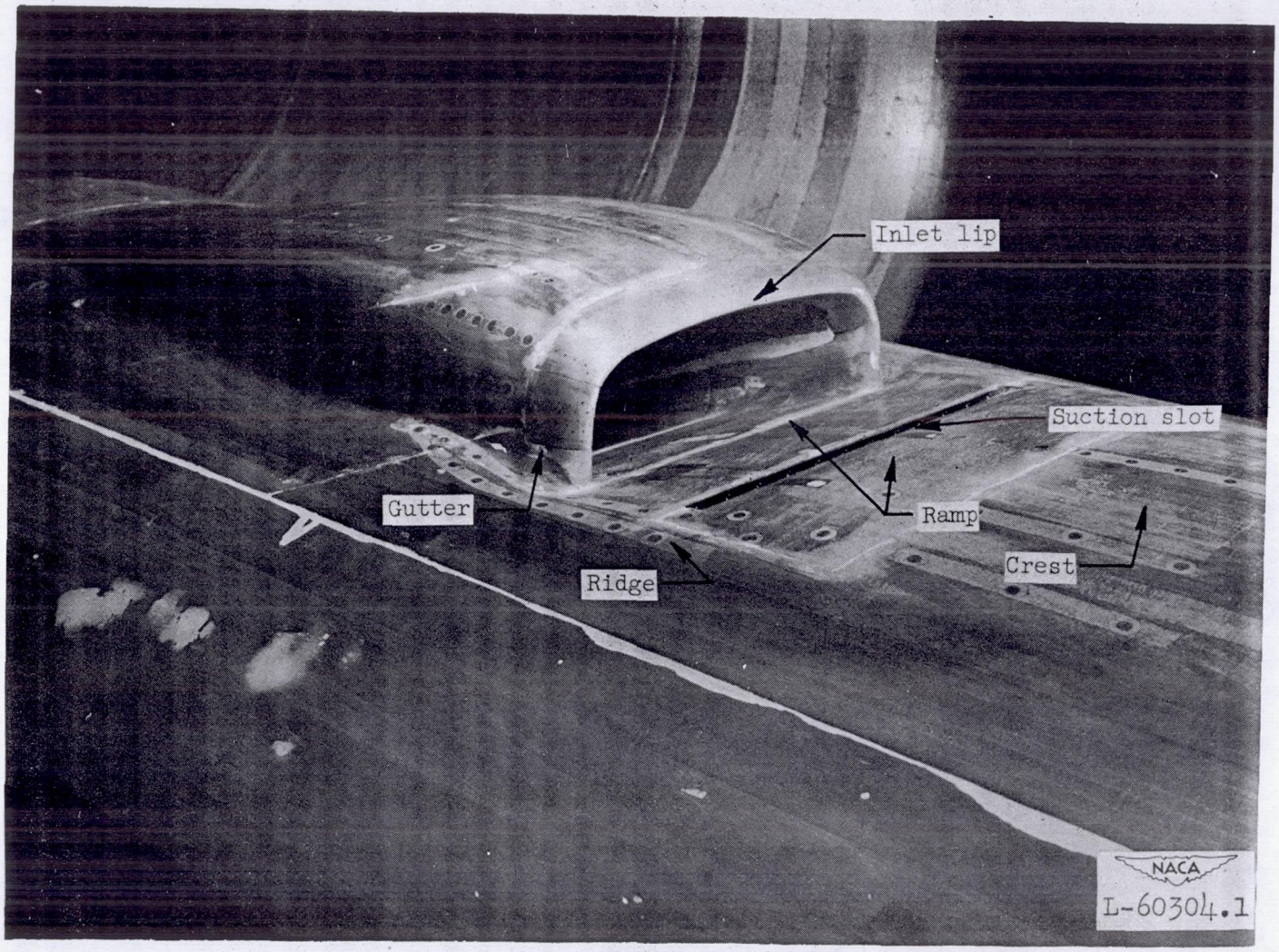


Figure 1.- Schematic diagram of test setup for semisubmerged inlet in open-throat tunnel.

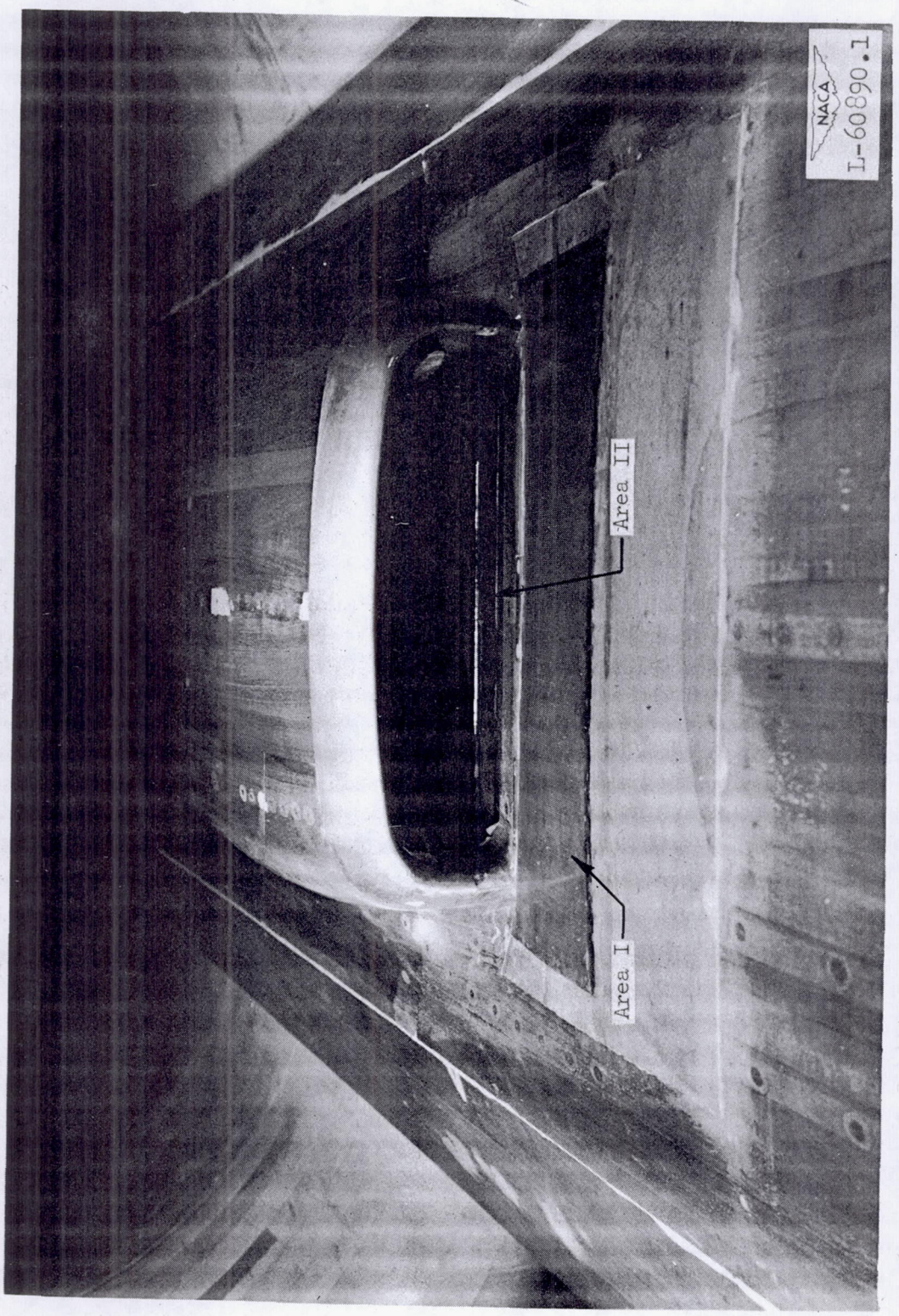
CONFIDENTIAL



(a) Slot III, 4 inches ahead of inlet.

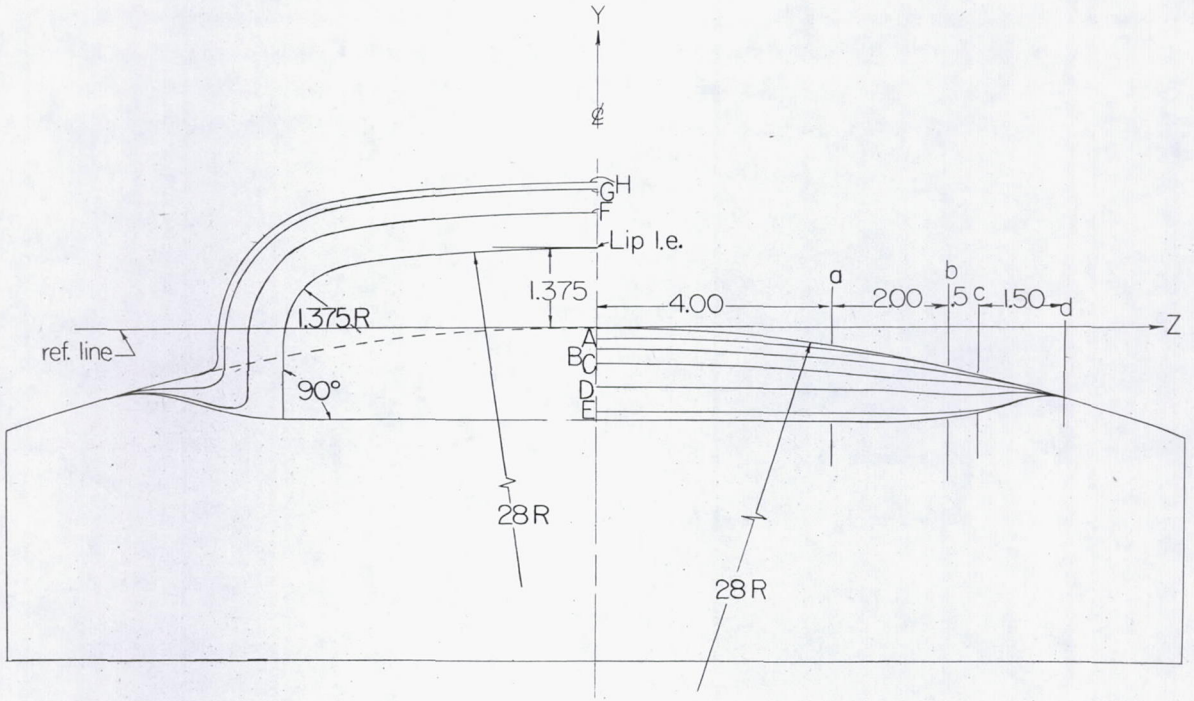
Figure 2.- Views of semisubmerged inlet installed in wind tunnel.

CONFIDENTIAL

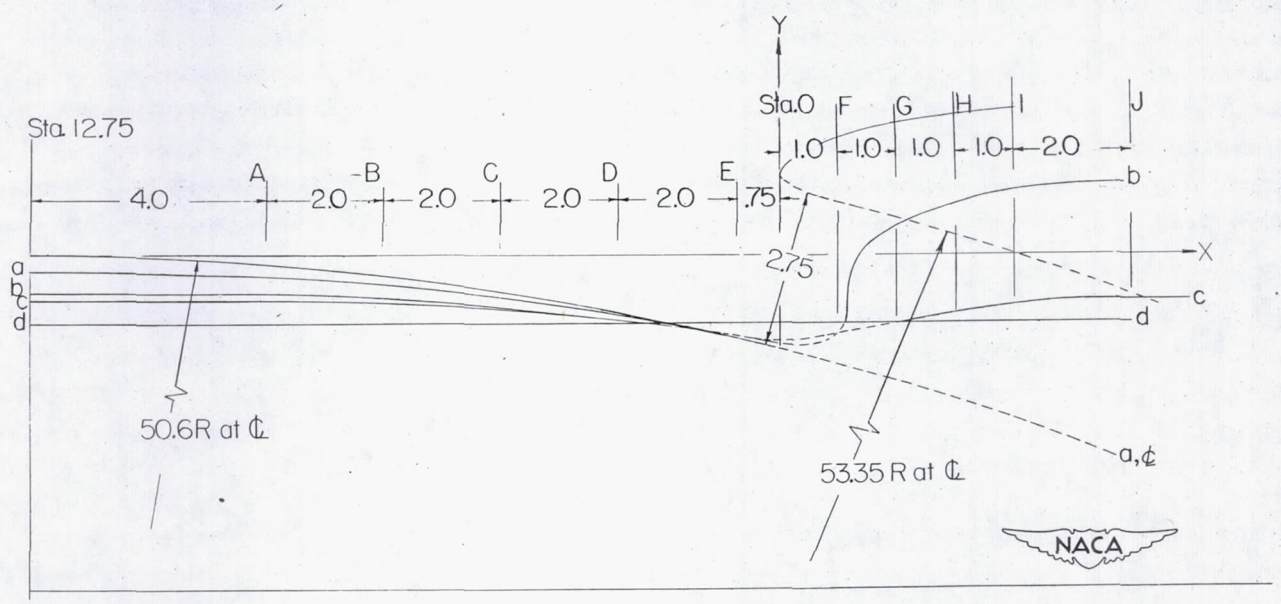


(b) Area suction, area I and area II.

Figure 2.- Concluded.

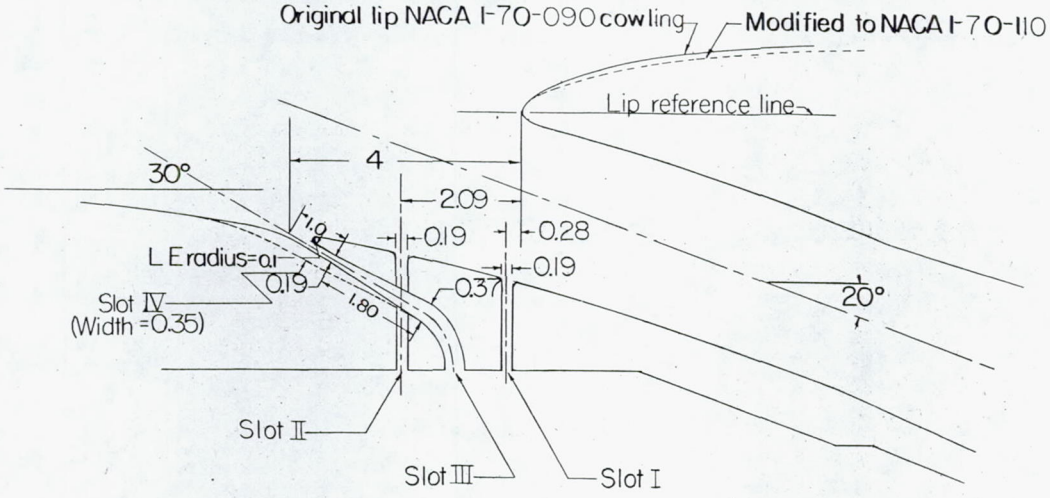


(a) Transverse lines of inlet lip and ramp.

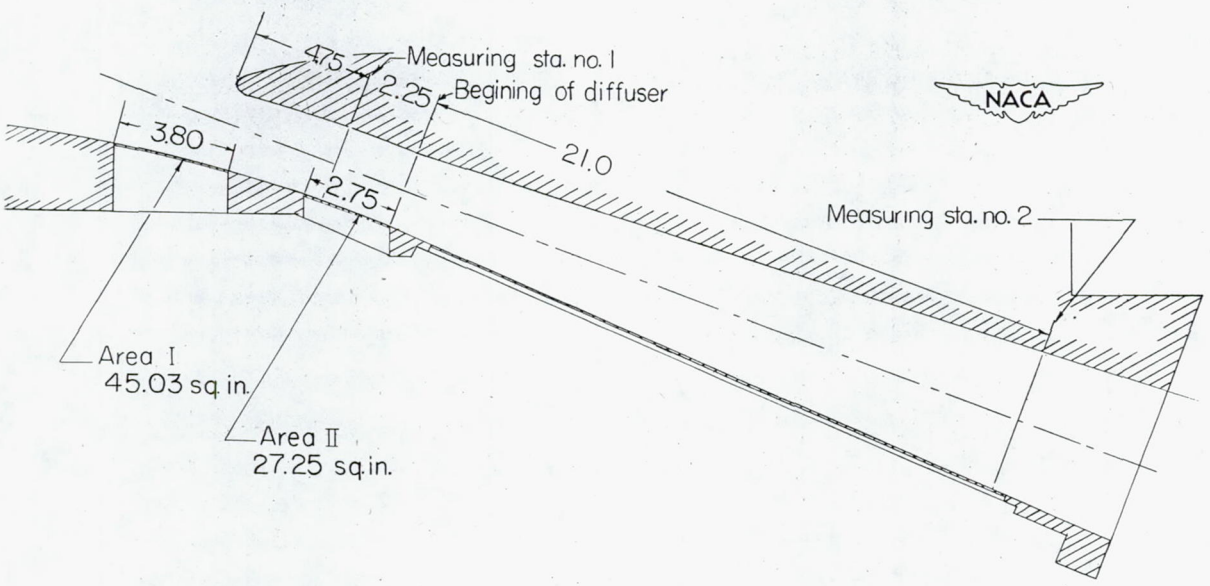


(b) Longitudinal lines of inlet ramp.

Figure 3.- Longitudinal and transverse lines of semisubmerged inlet. All dimensions are in inches.

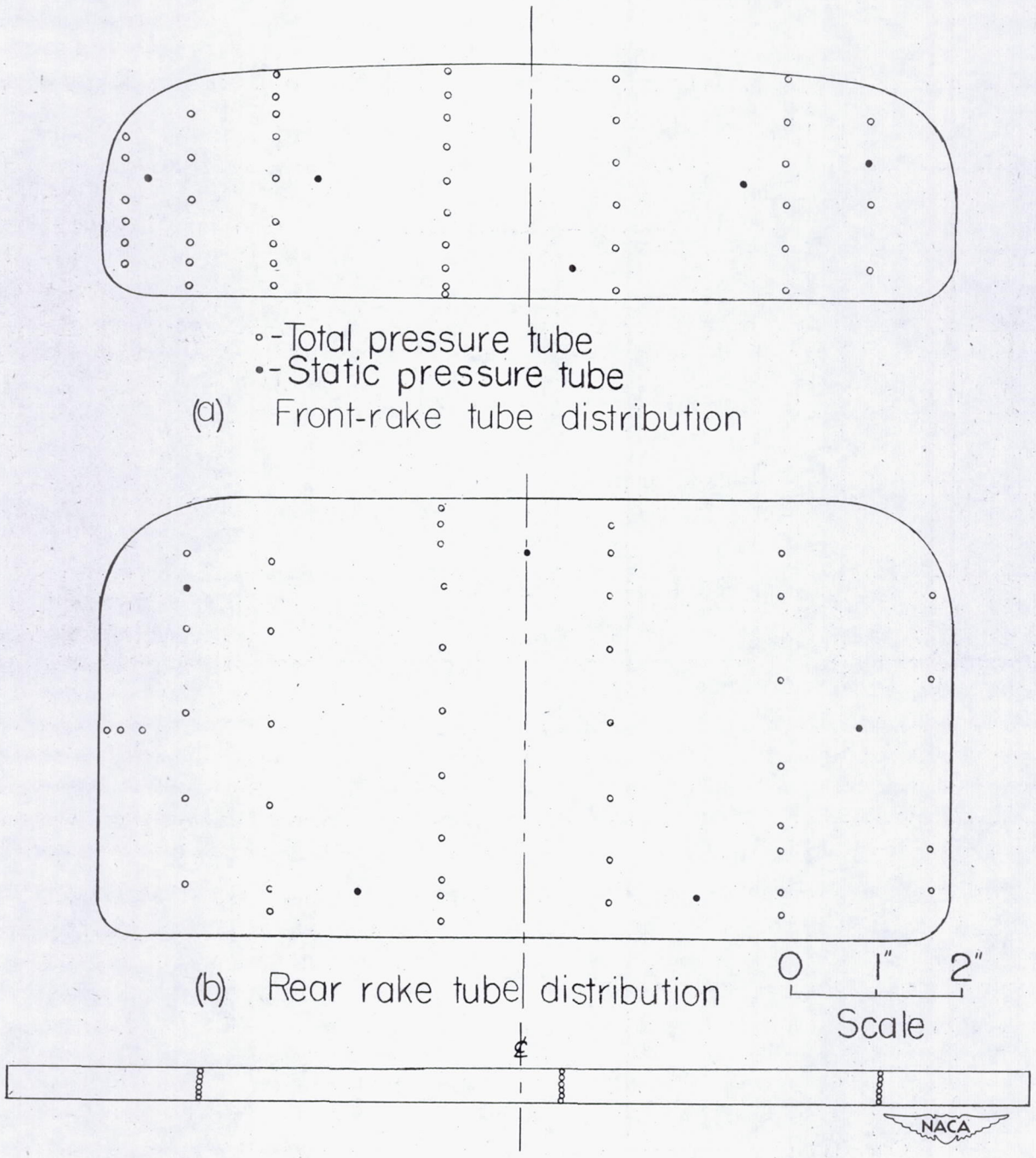


(a) Diagram showing different slot locations and lip shapes tested.



(b) Diagram showing location of porous areas tested.

Figure 4.- Diagrams showing slot and area locations.



(c) Slot-rake tube distribution.

Figure 5.- Locations of the pressure tubes in the main duct and in the boundary-layer slot.

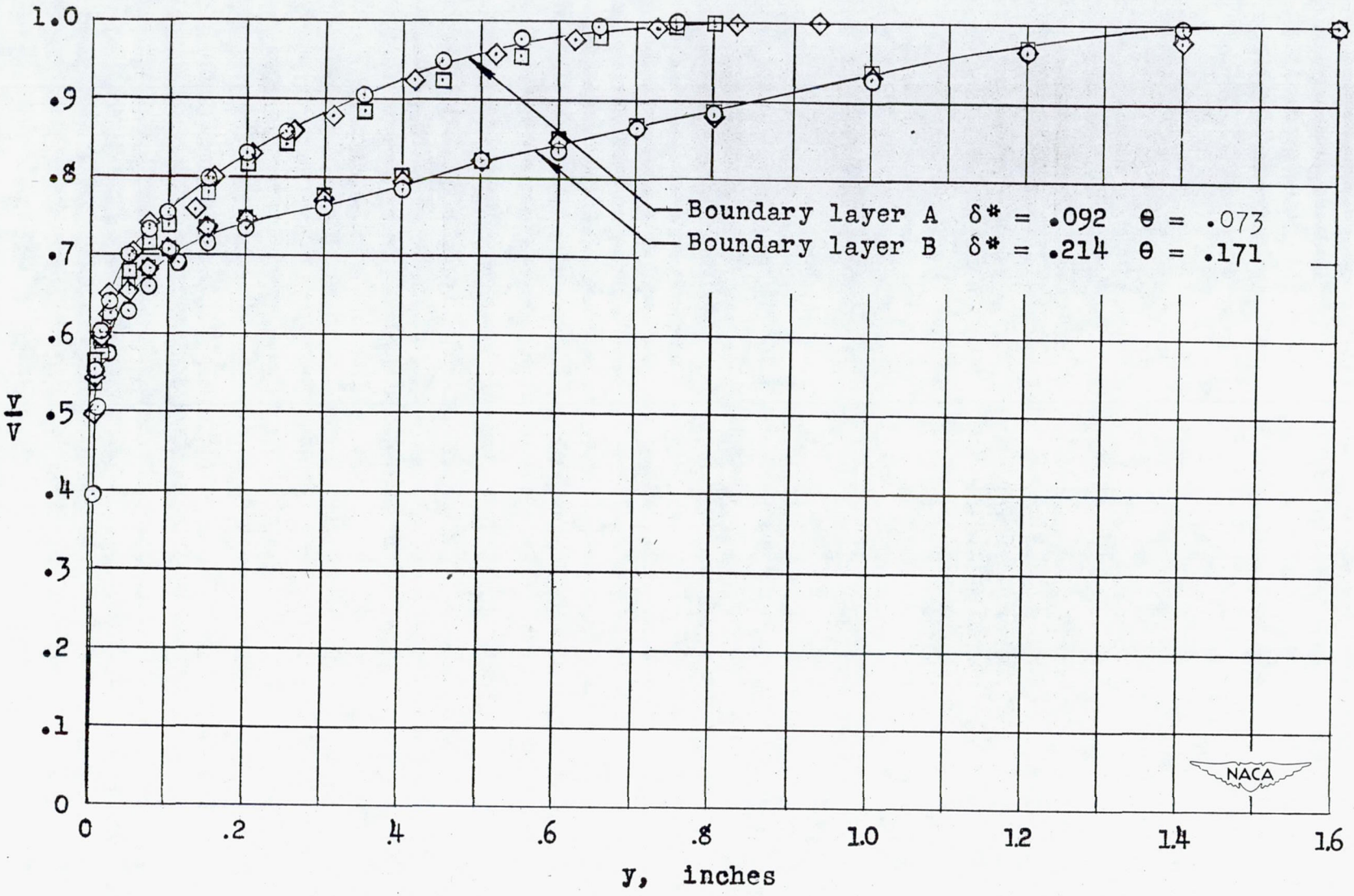


Figure 6.- Boundary-layer velocity profiles 14.5 inches ahead of inlet.

CONFIDENTIAL

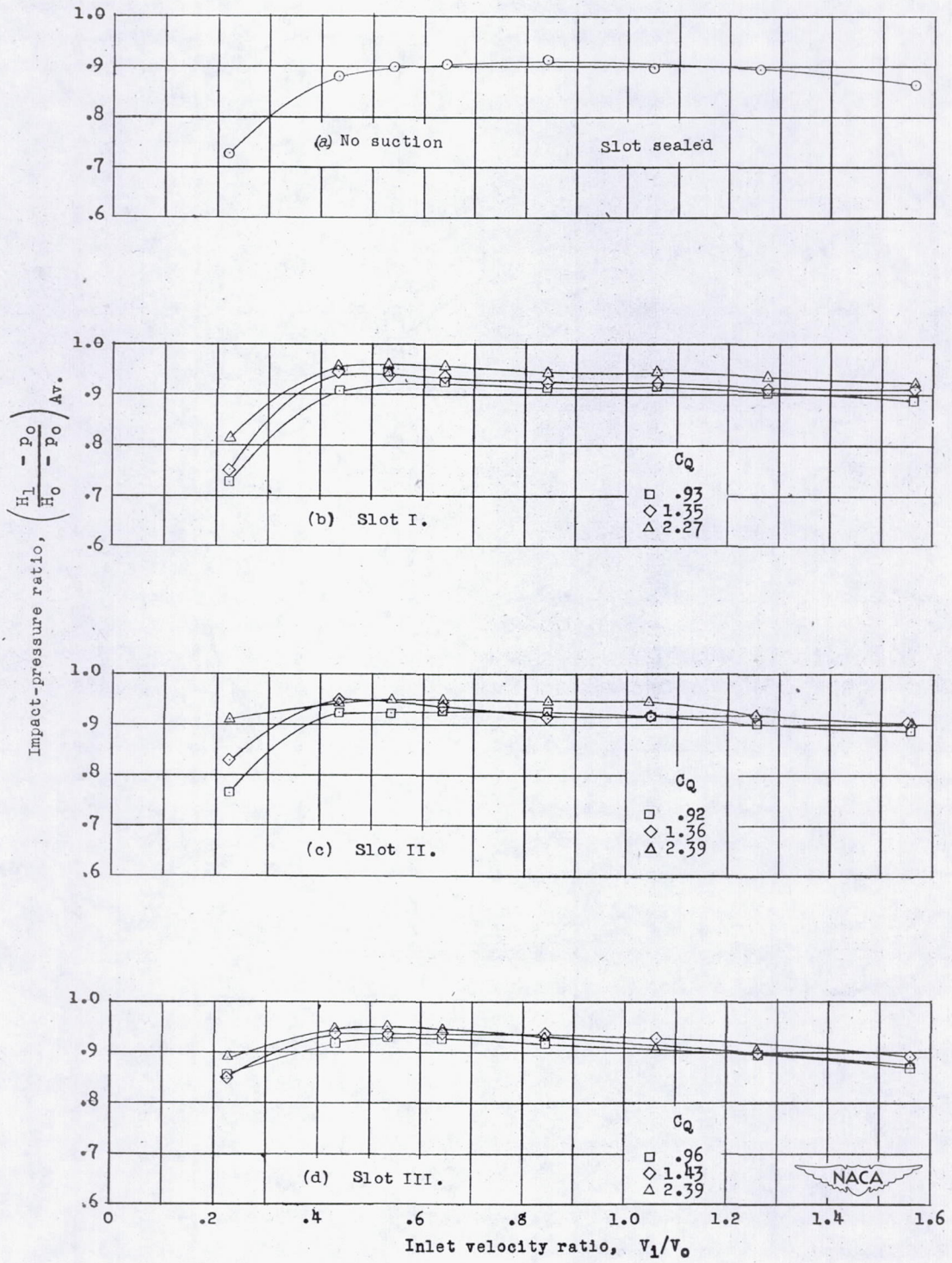
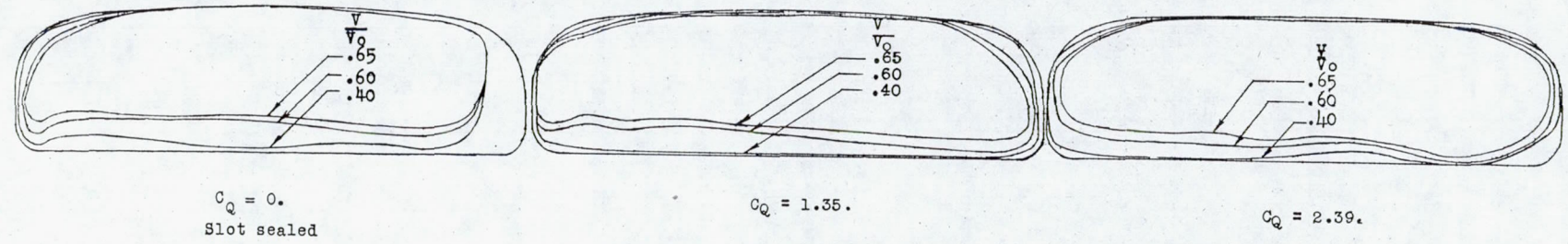
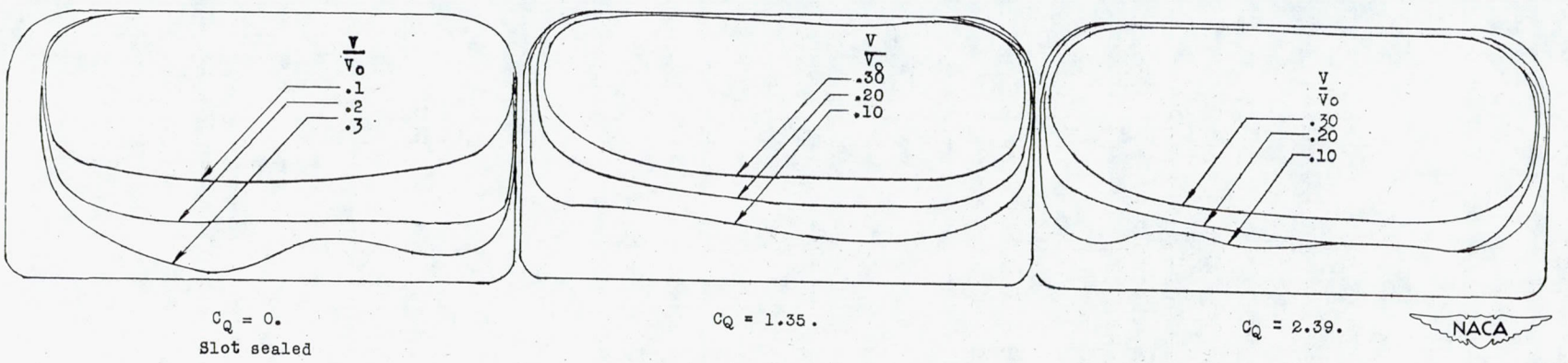


Figure 7.- Impact-pressure ratio at front measurement station.



(a) Front measurement station.



(b) Rear measurement station.

Figure 8.- Velocity contours of front and rear measurement stations; slot III, $\frac{V_i}{V_o} = 0.6$.

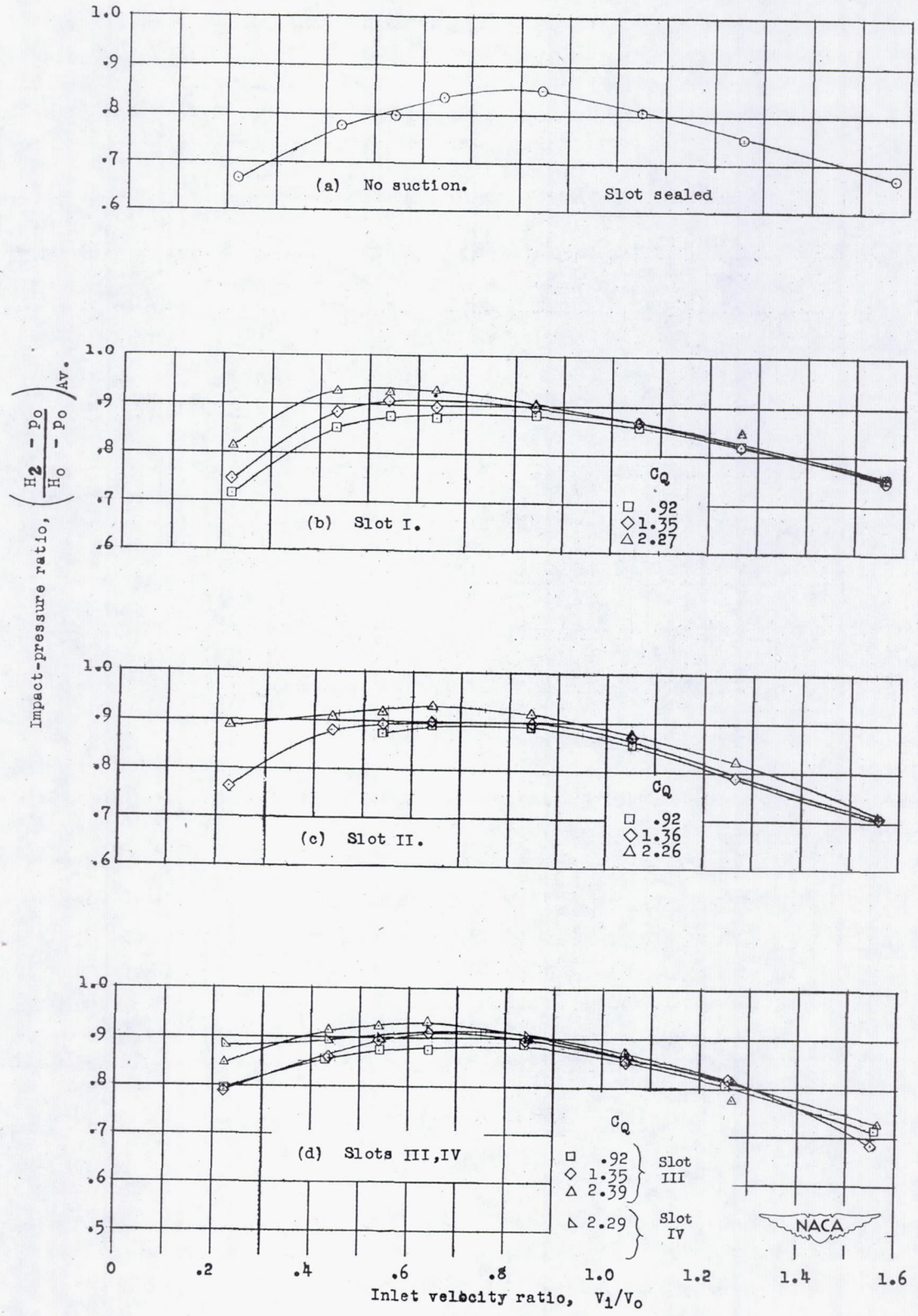


Figure 9.- Impact-pressure ratio at rear measurement station.

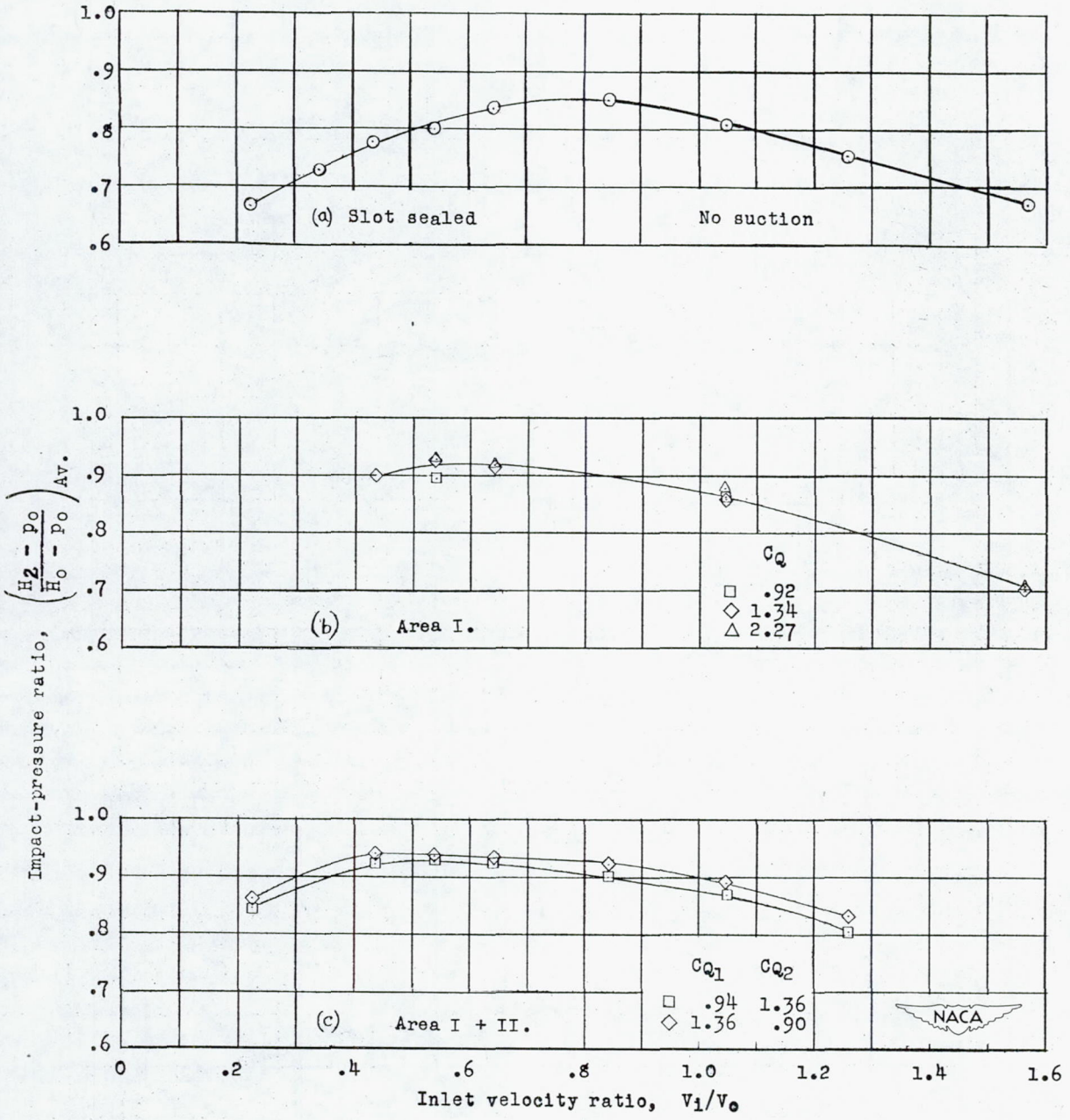


Figure 10.- Impact-pressure ratio at rear measurement station with area suction.

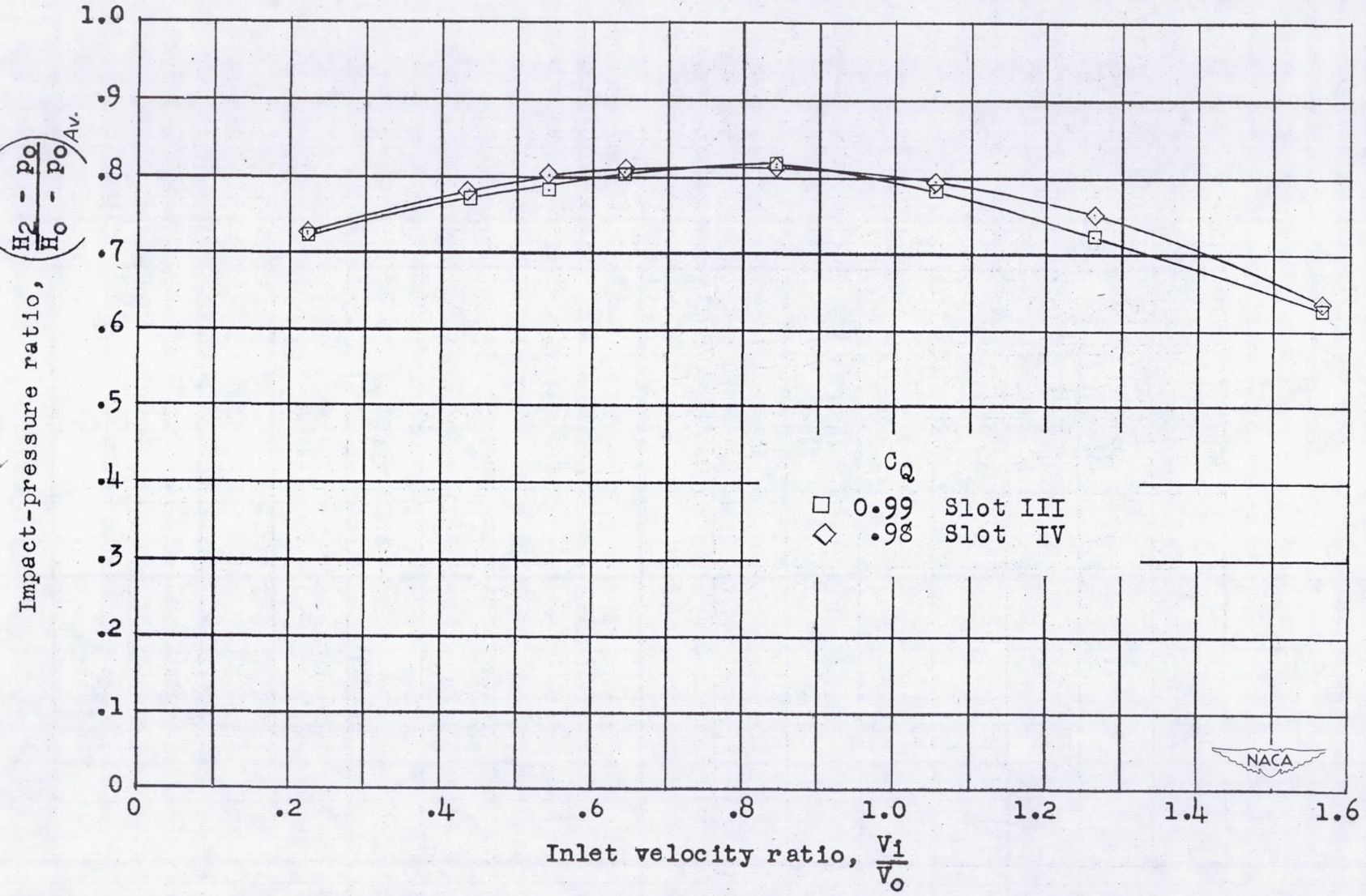
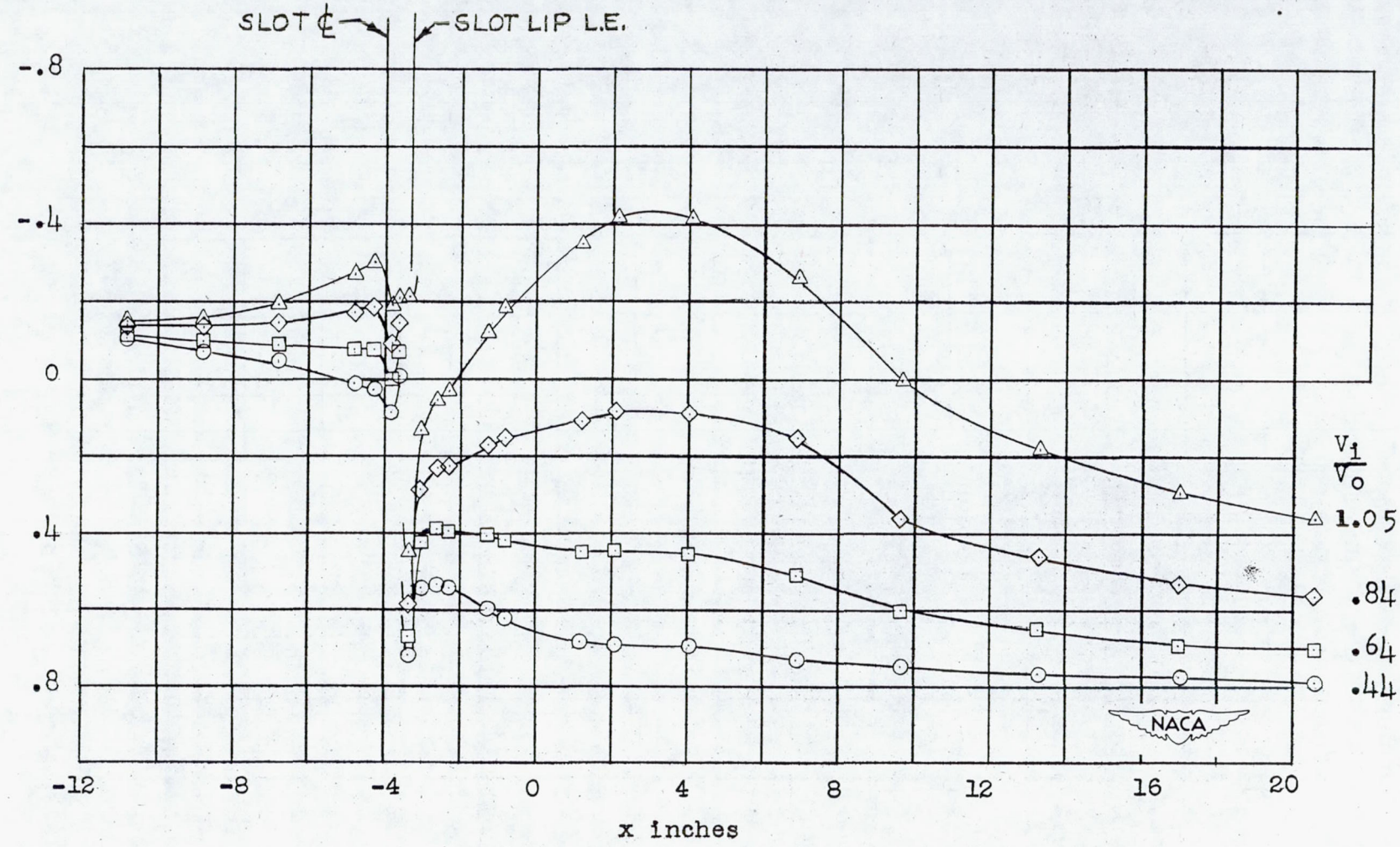
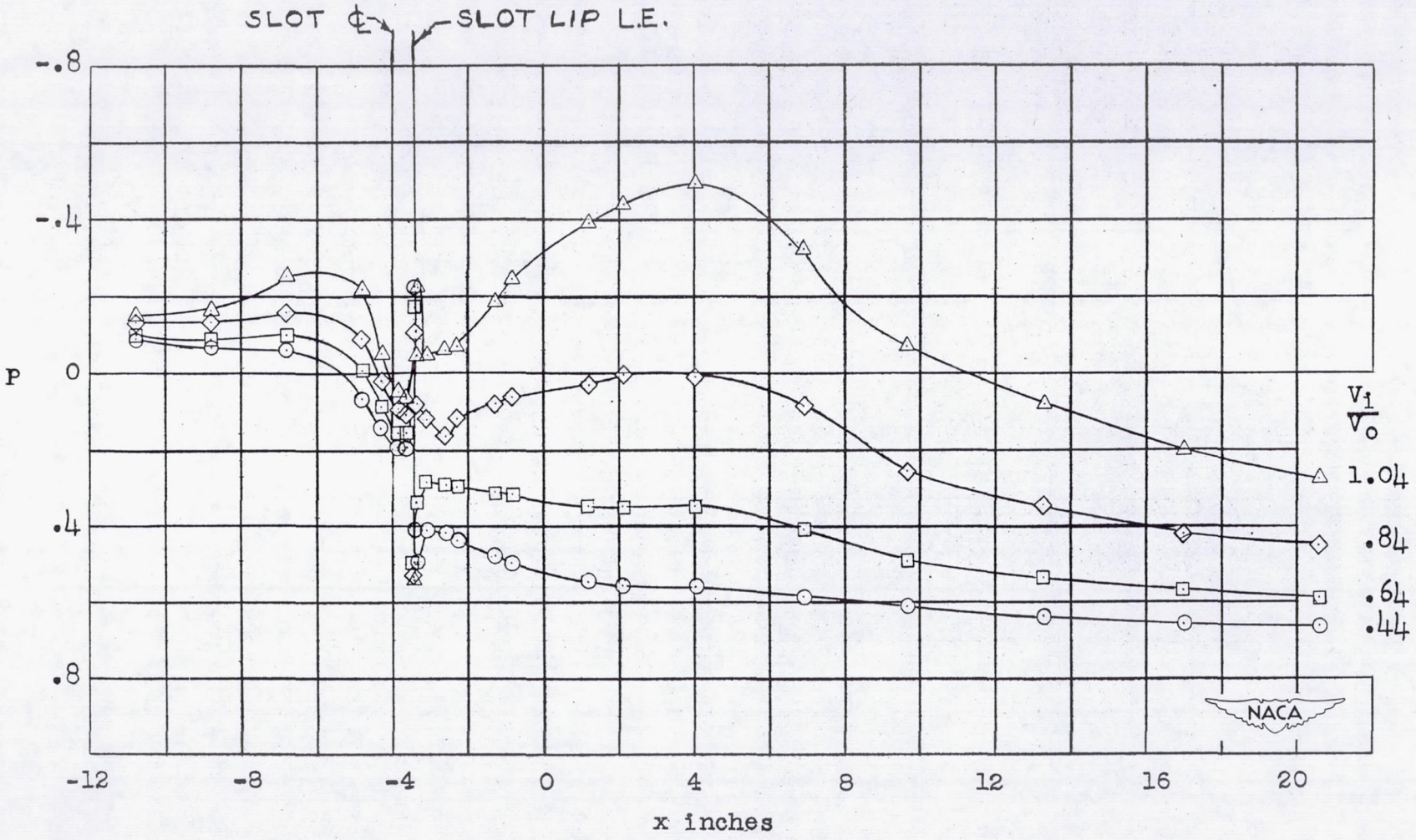


Figure 11.- Impact-pressure ratio at rear measurement station with boundary layer B. Slots III and IV.



(a) Slot III, C_Q = 2.39.

Figure 12.- Distribution of surface pressure along ramp and duct bottom.



(b) Slot IV, C_Q = 2.29.

Figure 12.- Continued.

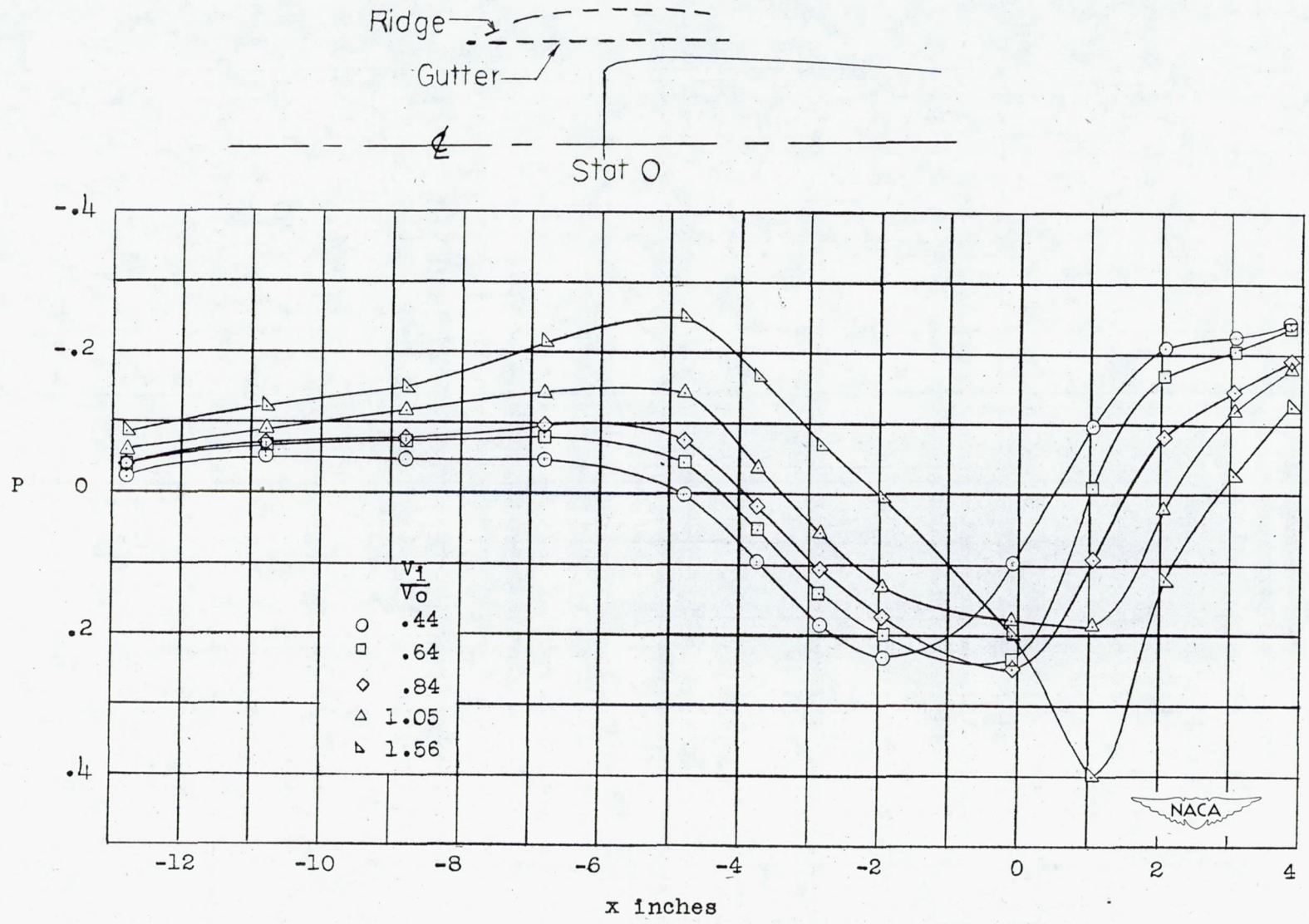
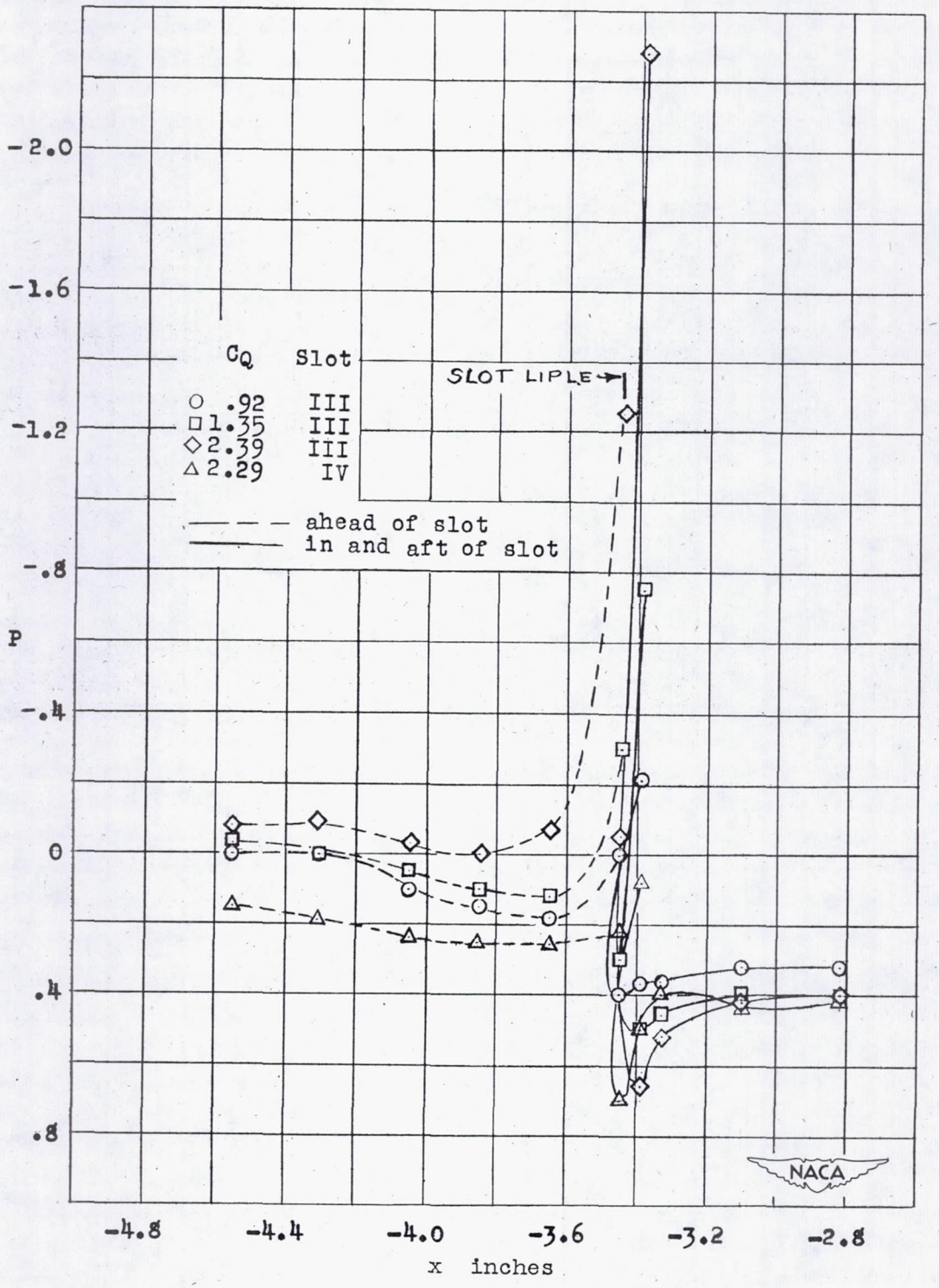


Figure 13.- Distribution of surface pressure in gutter. Slot IV; $C_Q = 2.29$.



(c) Slots III and IV, $\frac{V_i}{V_o} = 0.6$.

Figure 12.- Concluded.

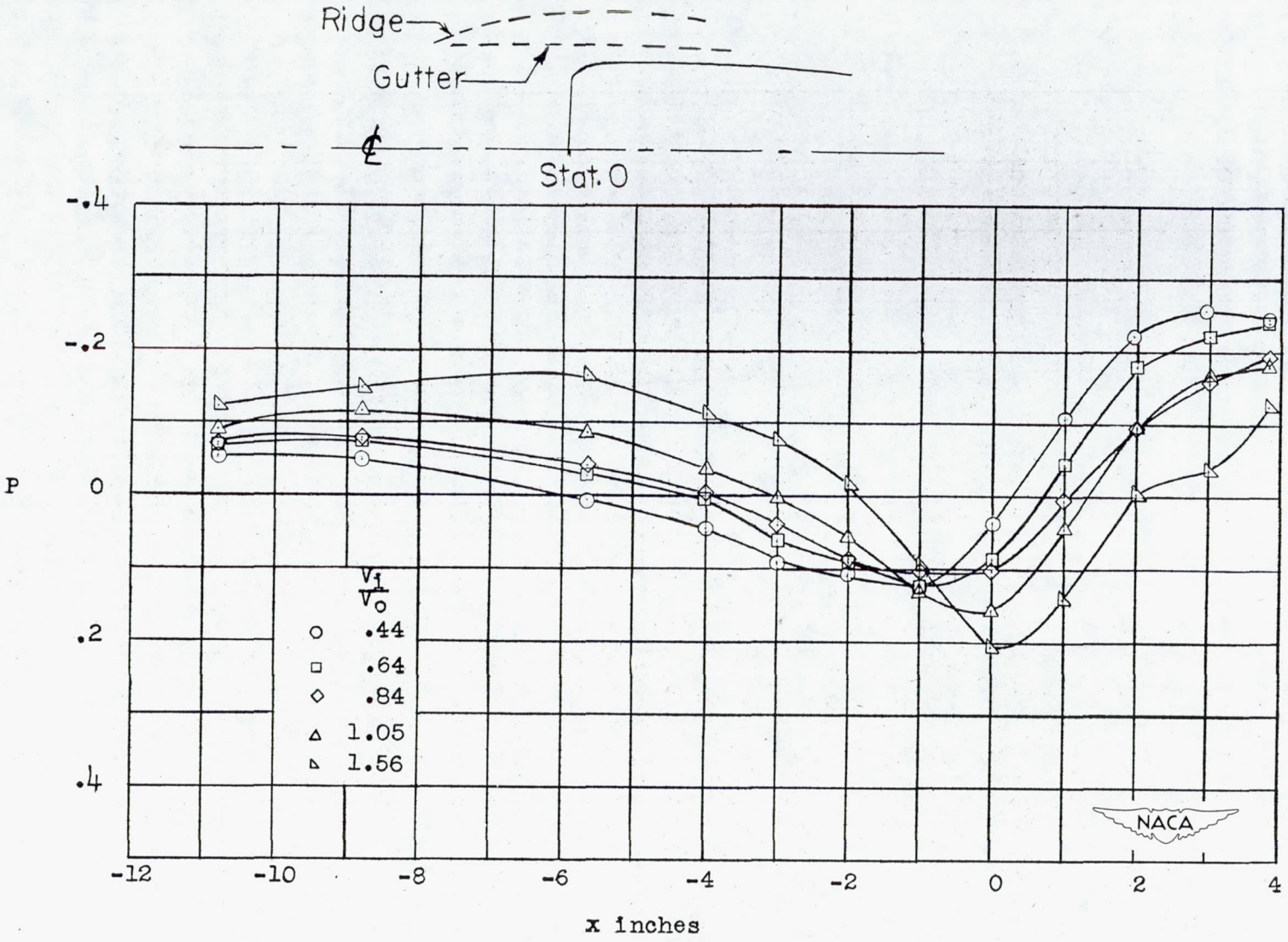
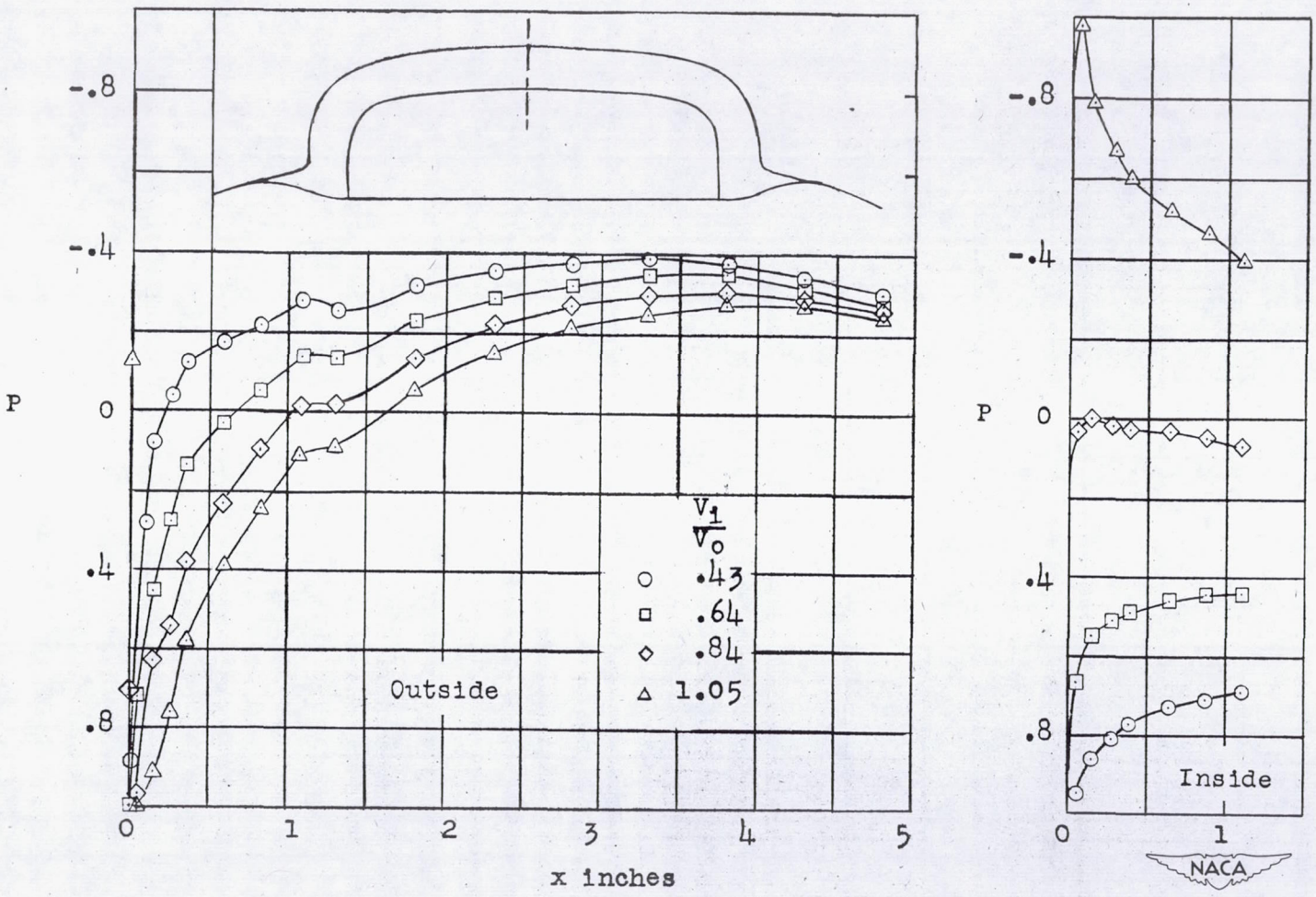


Figure 14.- Distribution of surface pressure on ridge. Slot IV; $C_Q = 2.29$.

CONFIDENTIAL

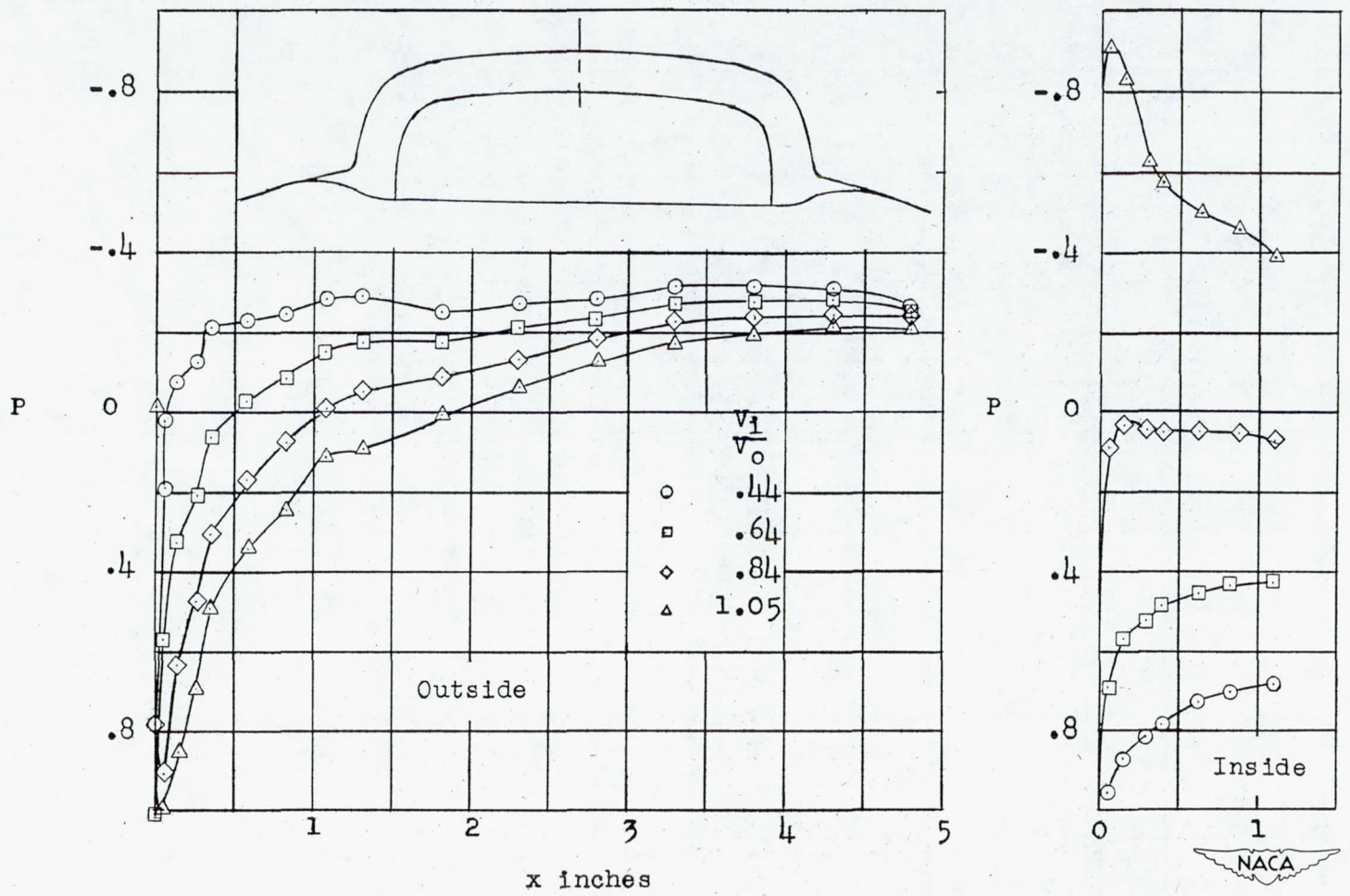


(a) Original lip center line. C_Q = 2.36; slot III.

Figure 15.- Distribution of surface pressure on inlet lip.

CONFIDENTIAL

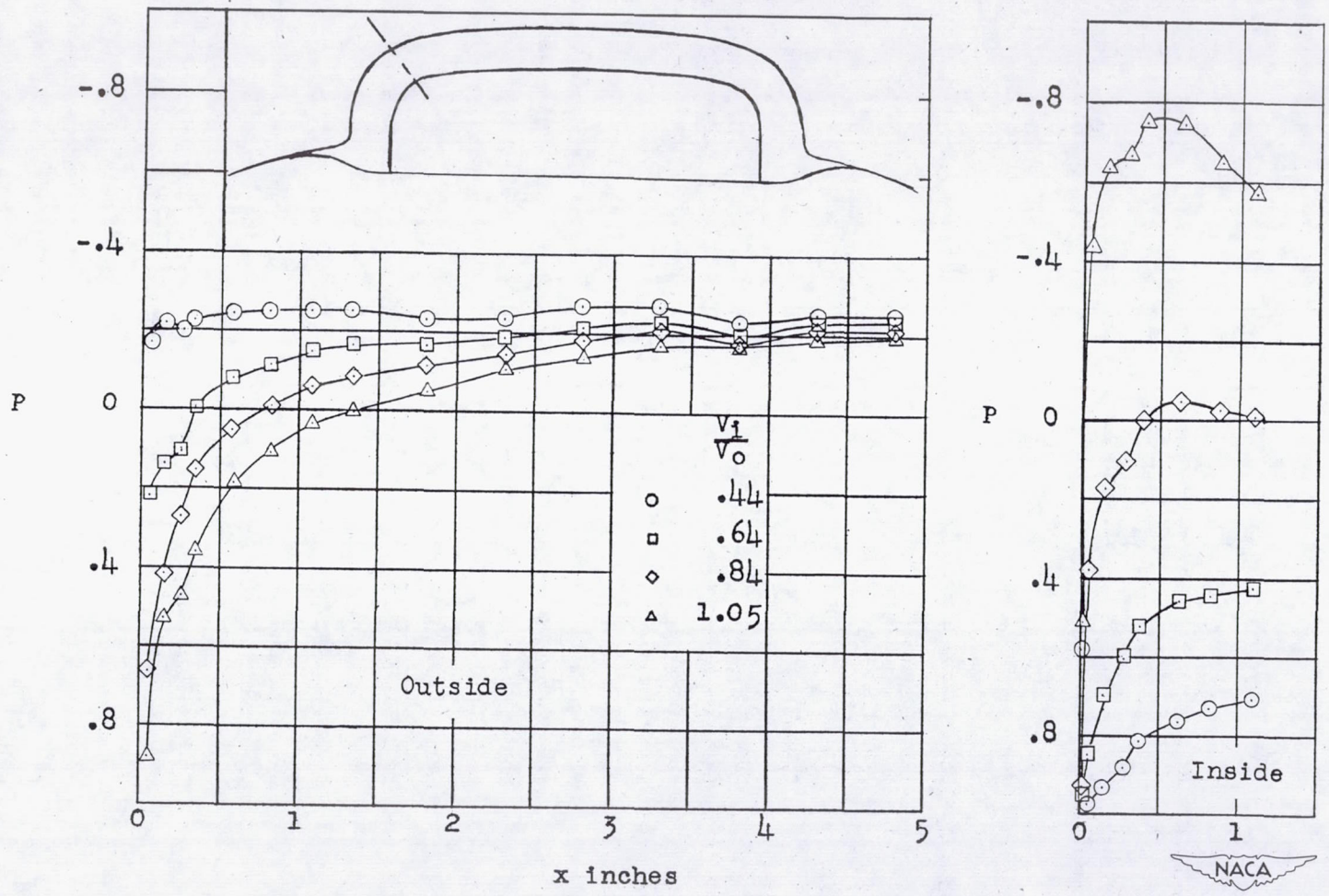
CONFIDENTIAL



(b) Modified lip center line. C_Q = 2.39; slot IV.

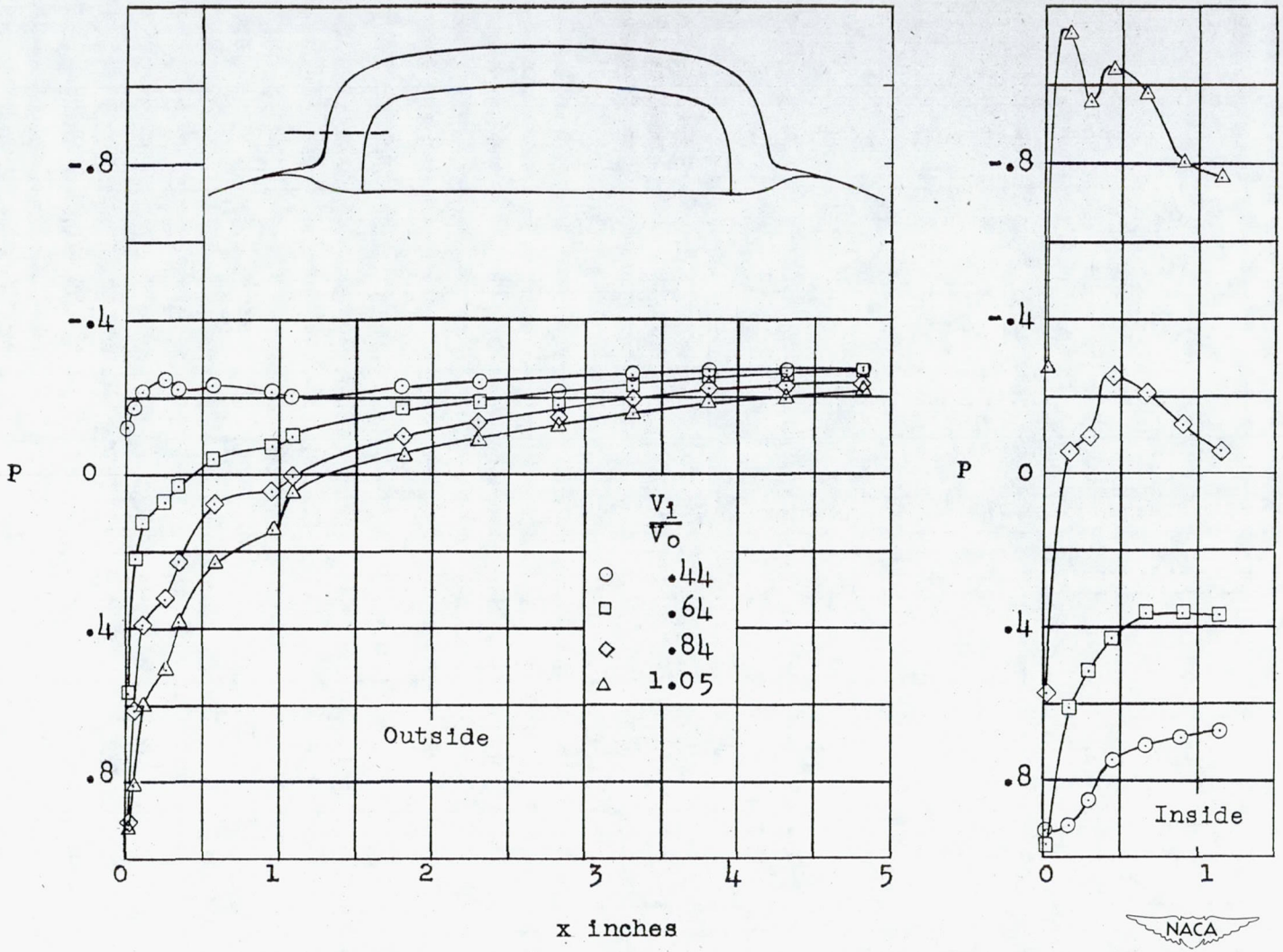
Figure 15.- Continued.

CONFIDENTIAL



(c) Top corner of modified lip. C_Q = 2.39; slot IV.

Figure 15.- Continued.



(d) End section of modified lip. C_Q = 2.39; slot IV.

Figure 15.- Concluded.

CONFIDENTIAL

CONFIDENTIAL

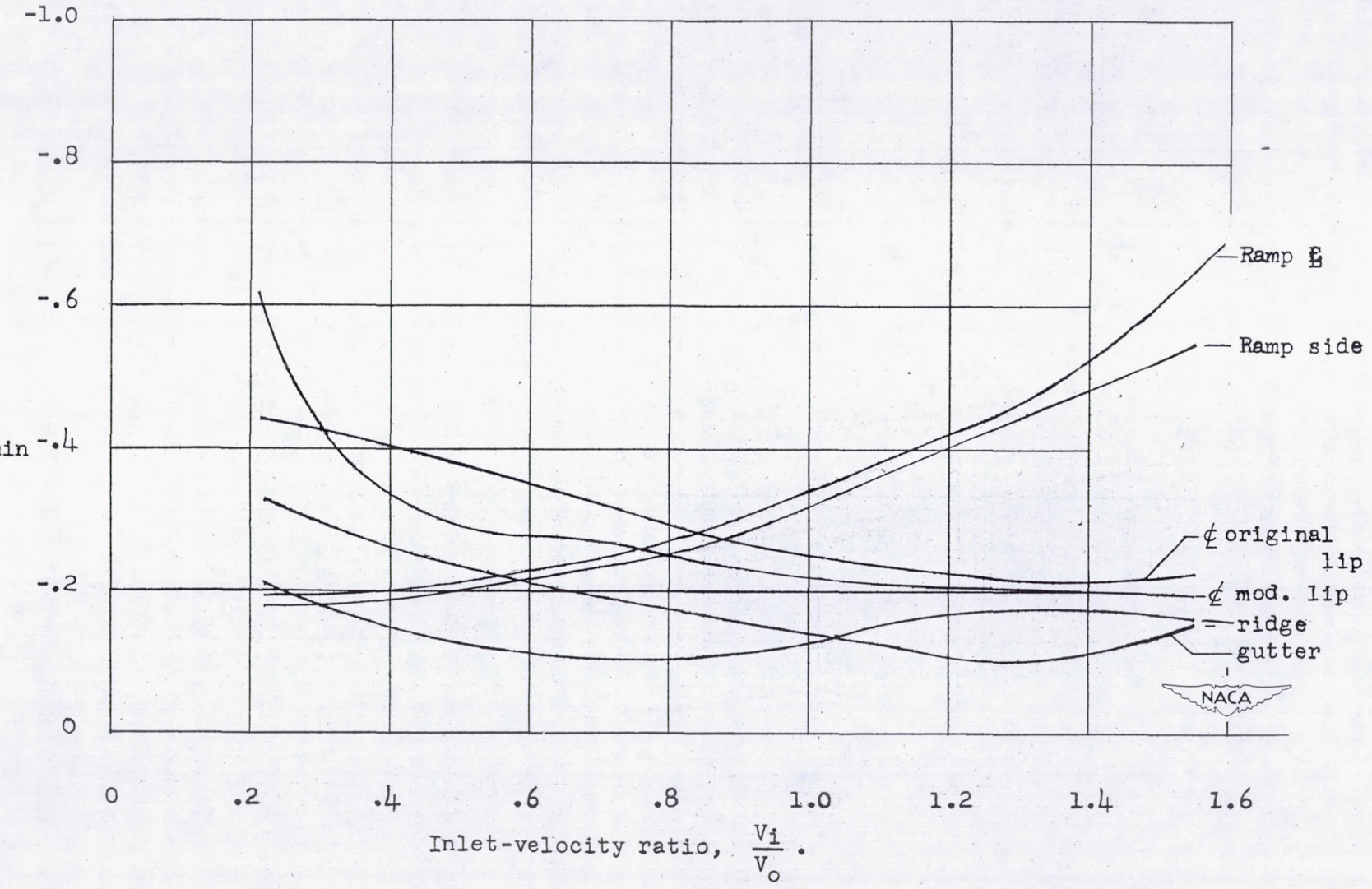


Figure 16.- Variation with inlet-velocity ratio of minimum surface pressure. Slot IV; C_Q = 2.29.

CONFIDENTIAL

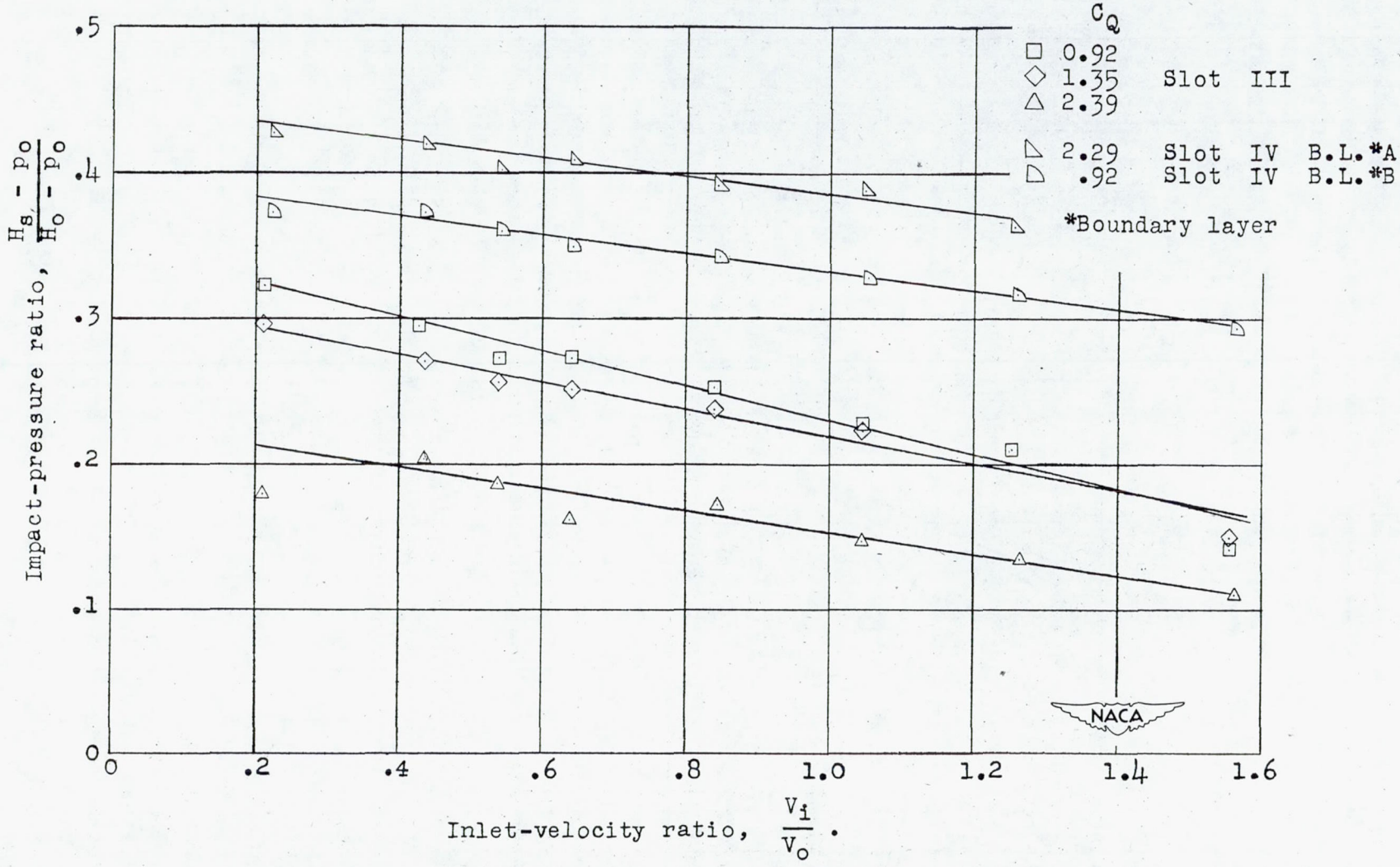


Figure 17.- Impact-pressure ratio in slot. Slot III and slot IV.

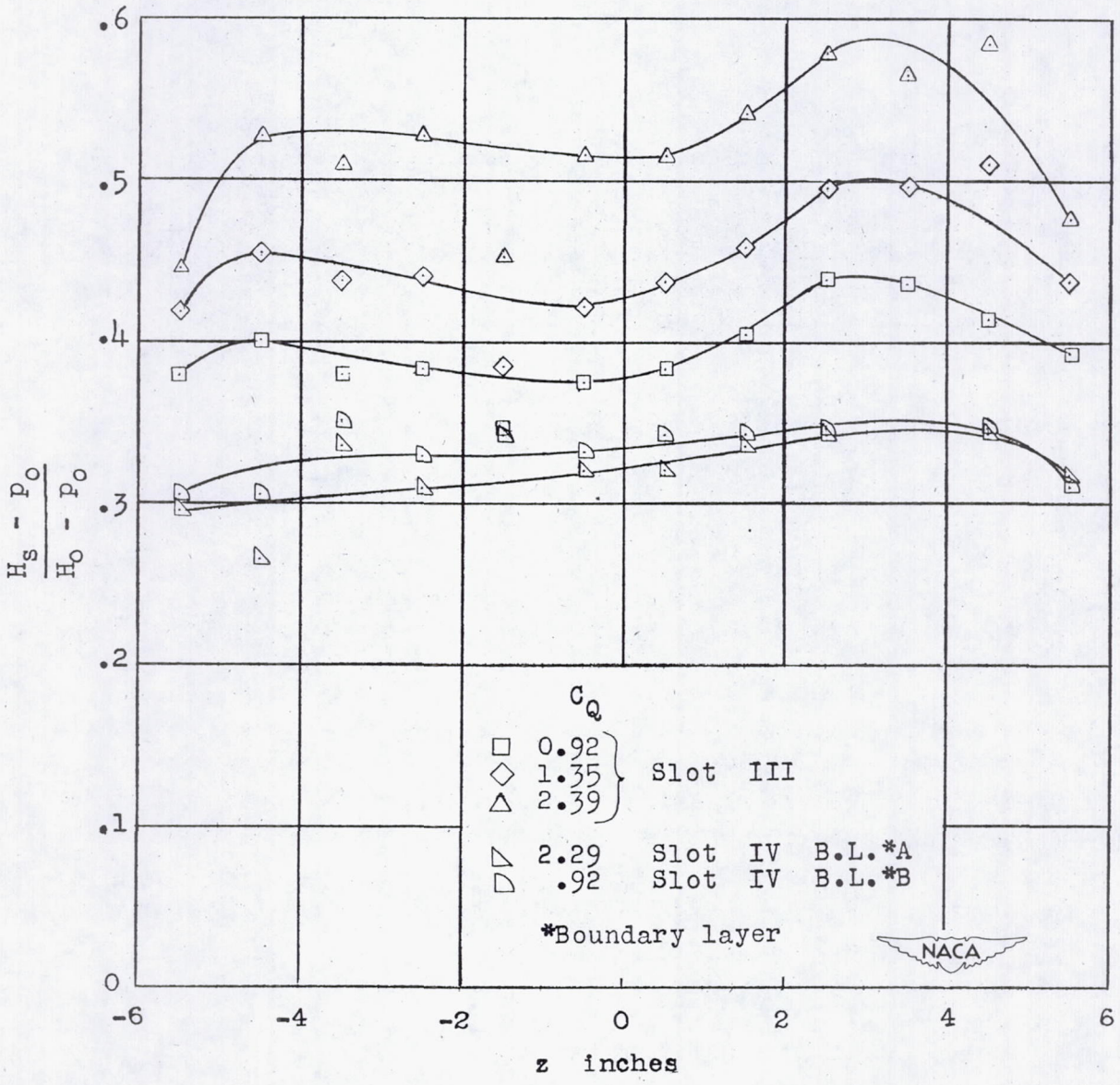


Figure 18.- Spanwise variation of impact-pressure ratio at slot entrance.

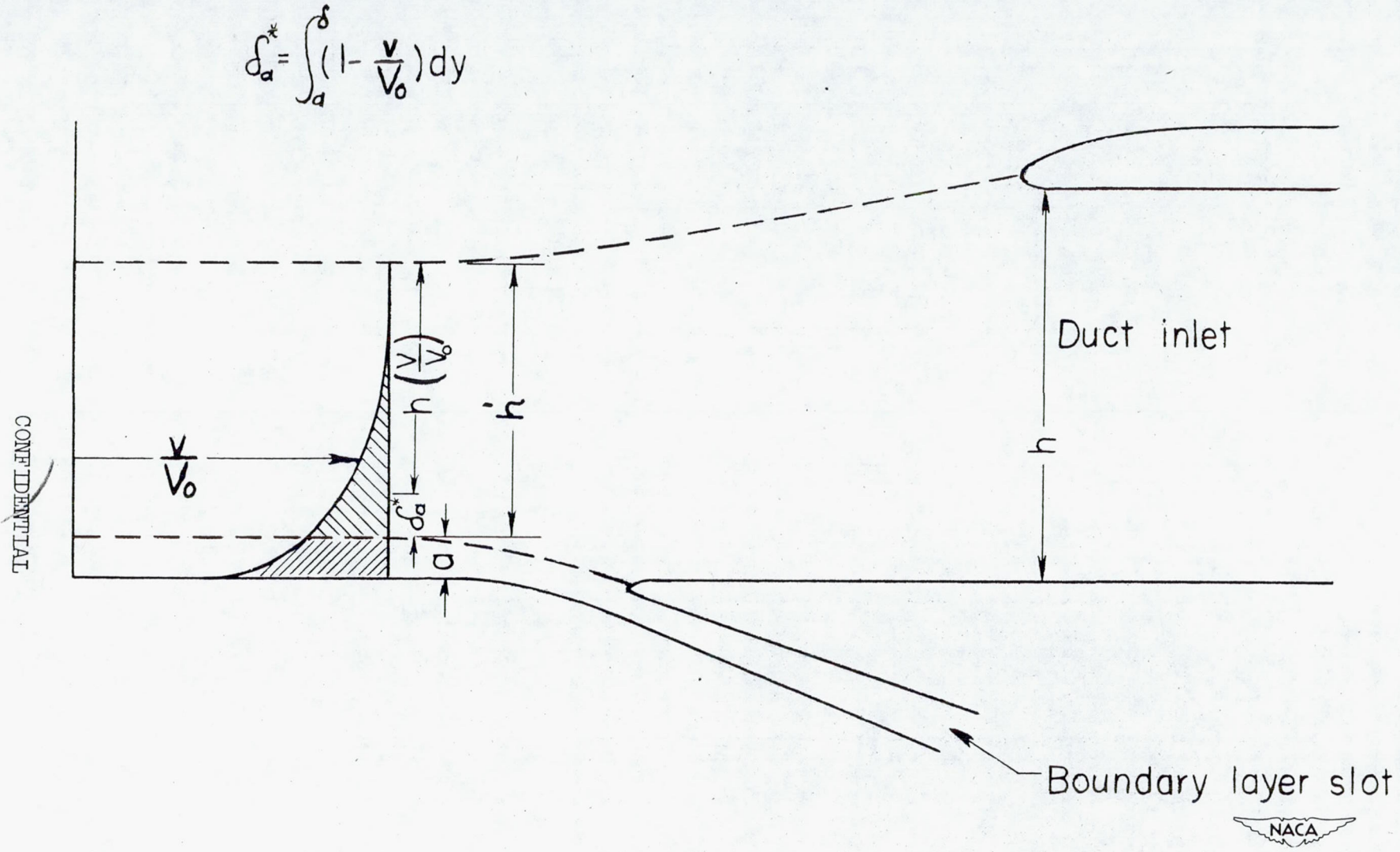


Figure 19.- Definition of quantities used in calculation of theoretical upper limit of impact-pressure ratio.

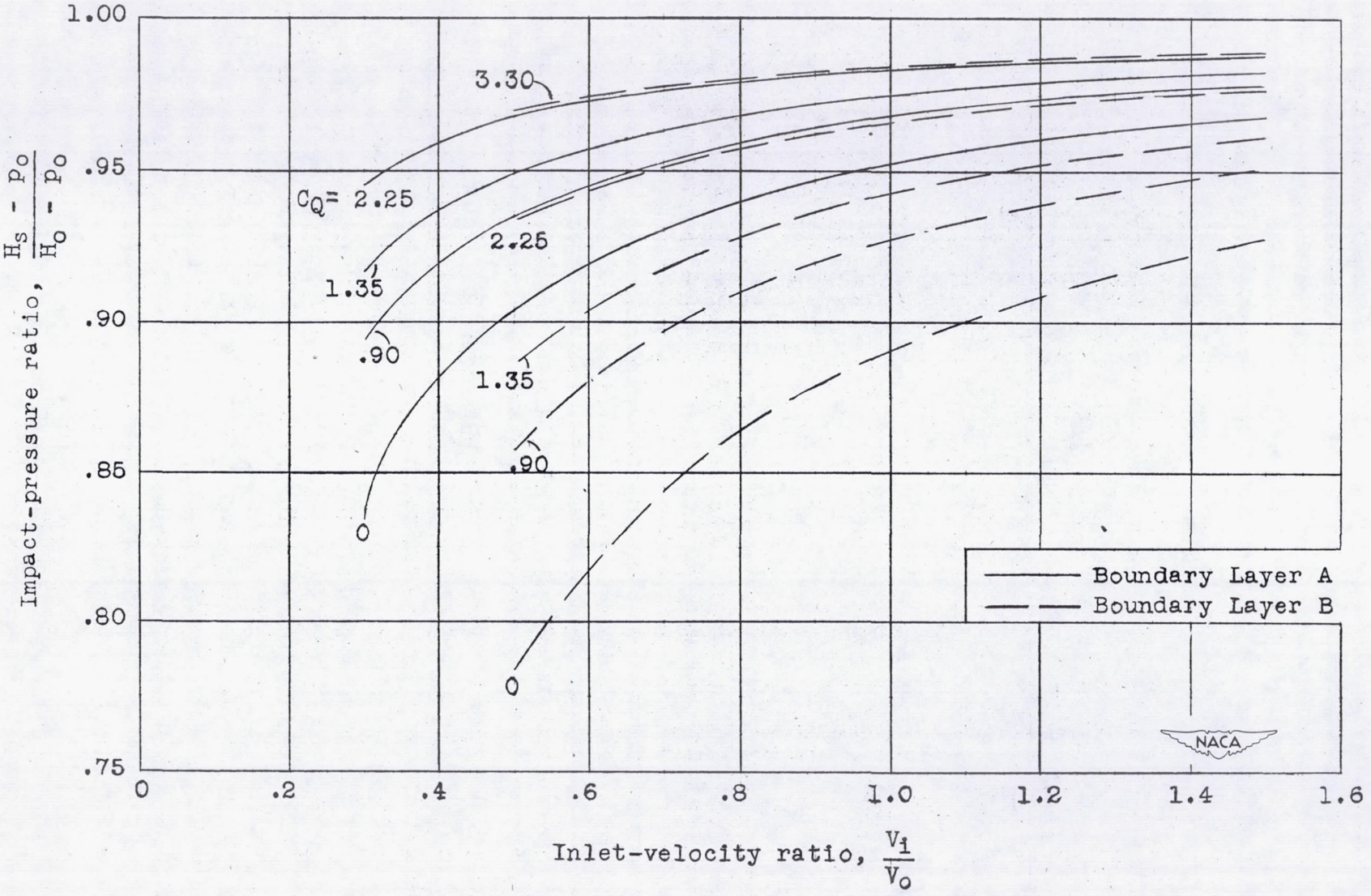
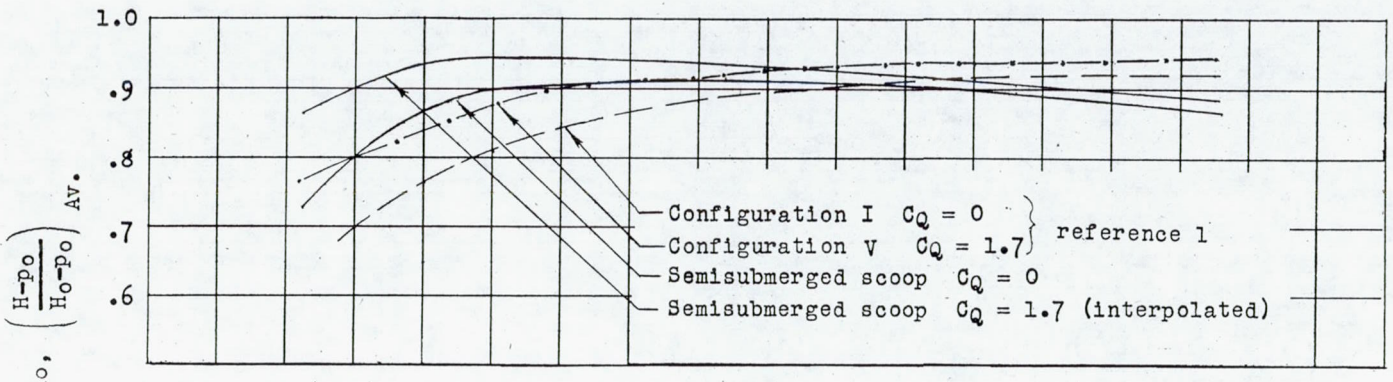
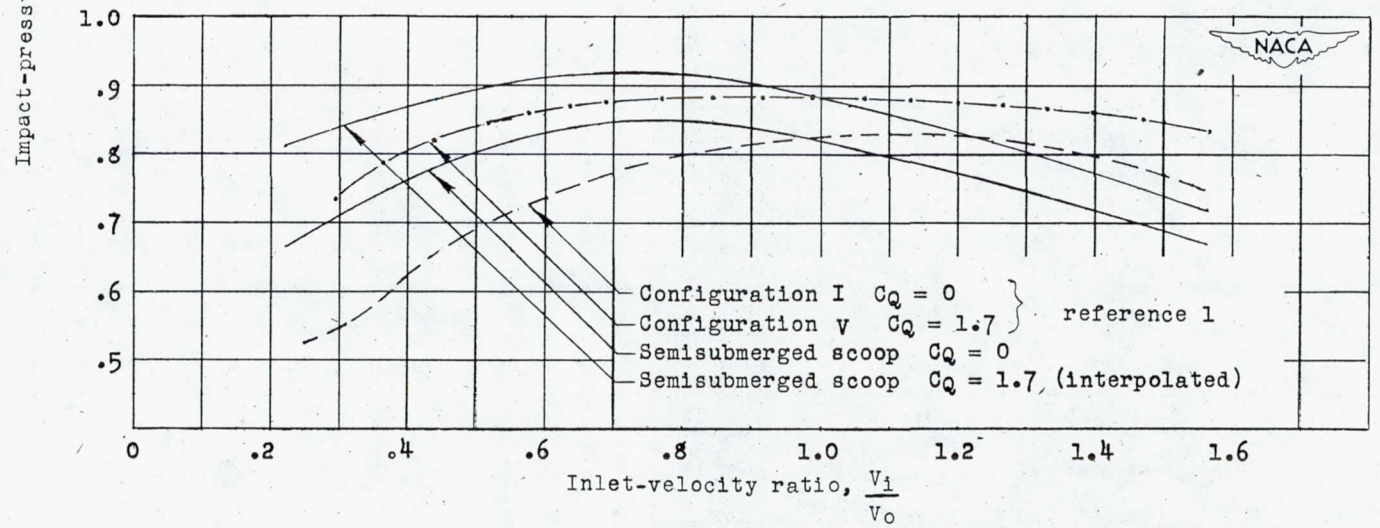


Figure 20.- Calculated upper limit of impact-pressure ratio at inlet. Boundary layer A and boundary layer B.

CONFIDENTIAL



(a) Front measurement station.



(b) Rear measurement station.

Figure 21.- Comparison of impact-pressure ratio of semisubmerged scoop with that of submerged scoop of reference 1.

CONFIDENTIAL